Busby *et al. Fire Ecology* (2023) 19:58
https://doi.org/10.1186/s42408-023-00219-x

Fire Ecology

ORIGINAL RESEARCH

Open Access

Inventory analysis of fire effects wrought by wind-driven megafires in relation to weather and pre-fire forest structure in the western Cascades

Sebastian U. Busby[1*], Angela M. Klock[1] and Jeremy S. Fried[1]

Abstract

Background Six synchronous, wind-driven, high severity megafires burned over 300,000 hectares of mesic temperate forest in the western Cascades of NW Oregon and SW Washington states in early September 2020. While remote sensing data has been utilized to estimate fire severity across the fires, assessments of fire impacts informed by field observations are missing. We compiled field measurement data, pre- and post-fire, from a statistically representative sample of existing forest inventory analysis (FIA) plots, to estimate stand-level fire effects indices that describe (1) tree survival and its implications for carbon emissions, (2) effects on tree crowns, and (3) effects on soils. Field observations were analyzed in relation to fire weather when plots burned and to evaluate accuracy of remotely sensed burn severity classifications.

Results Wind speed strongly interacted with tree size and stand age to influence tree survival. Under high fuel aridity but light winds, young stands composed of small trees, found primarily on private lands, exhibited a much lower survival rate than older stands composed of medium to large trees, found primarily on federal lands. Under moderate to high winds, poor tree survival was characteristic of all forest structures and ownerships. Fire impacts on tree crowns were strongly related to wind speed, while fire impacts on soils were not. These fires transferred nearly 70 MMT CO_2e from wood in live and growing trees to a combination of immediate smoke and carbon emissions, plus delayed emissions from dead wood, that will release most of the embodied carbon over the next few decades. These emissions will exceed all 2020 anthropogenic emissions in Oregon (64 MMT CO_2e). Substantial discrepancies were observed between two remotely sensed burn severity products, BAER-SBS and MTBS-TC, and field observed soil organic matter cover and tree mortality, respectively.

Conclusions Post-fire FIA plot remeasurements are valuable for understanding fire's impact on forest ecosystems and as an empirical basis for model validation and hypothesis testing. This continuous forest inventory system will compound the value of these post-fire remeasurements, enabling analysis of post-fire forest ecosystem trajectories in relation to both immediate fire impacts and pre-fire conditions.

Keywords Fire effects, Fire weather, Wind speed, Megafire, Temperate conifer forest, Western cascades, Forest inventory, Tree mortality, Carbon dynamics, Burn severity classification accuracy

*Correspondence:
Sebastian U. Busby
sebastian.busby@usda.gov
Full list of author information is available at the end of the article

Resumen

Antecedentes Seis megaincendios sincrónicos de alta severidad y conducidos por el viento, quemaron más de 300 mil ha de bosques templados mésicos en las montañas *West Cascades* en el noreste de los estados de Oregón y el sudeste de Washington (EEUU) a principios de septiembre de 2020. Aunque los datos de sensores remotos han sido utilizados para estimar la severidad del fuego a través de diferentes incendios, éstos omiten la determinación de los impactos del fuego que provee la observación visual a campo. Compilamos datos de mediciones a campo previos y posteriores al incendio de una muestra estadísticamente representativa de inventarios existentes de análisis de parcelas (FIA), para estimar los índices de los efectos del fuego a nivel de rodal y que describen (1) la supervivencia de árboles y sus implicancias en las emisiones de carbono, (2) los efectos del fuego sobre las coronas de los árboles, y (3) los efectos del fuego sobre el suelo. Las observaciones de campo fueron analizadas sobre las parcelas y en relación con la meteorología al momento del incendio, y para evaluar la exactitud de la clasificación de la severidad mediante los sensores remotos.

Resultados La velocidad del viento interactuó de manera muy fuerte con el tamaño de los árboles y la edad del rodal en la supervivencia de los árboles. Bajo condiciones de alta aridez de los combustibles, pero vientos leves, los rodales de árboles jóvenes, encontrados primariamente en campos privados, exhibieron una mucho menor tasa de supervivencia que rodales más antiguos compuestos de árboles medianos a grandes, encontrados principalmente en tierras federales. Bajo vientos moderados a altos, una supervivencia muy pobre fue una característica encontrada en todas las estructuras y formas de tenencia de esos bosques. El impacto del fuego en las coronas de los árboles fue fuertemente relacionado con la velocidad del viento, mientras que ésta no tuvo relación con los impactos sobre el suelo. Estos incendios transfirieron cerca de 70 MMT de Carbono equivalente desde la biomasa viva y en combinación con el humo y emisiones inmediatas de carbono, más las emisiones retrasadas retenidas por la biomasa muerta y que se irán liberando en las próximas décadas. Estas emisiones excederán las emisiones antropogénicas ocasionadas en 2020 en Oregon (64 MMT CO2e). Discrepancias substanciales fueron observadas entre dos productos obtenidos de información de sensores remotos, BAER-SB y MTBS-TC, y las observaciones de campo sobre cobertura de materia orgánica y mortalidad de árboles, respectivamente.

Conclusiones La remedición de parcelas FIA post fuego son valiosas para entender el impacto del fuego en ecosistemas forestales como una base empírica para la validación de modelos y testeo de hipótesis. Este modelo de monitoreo continuo recompondrá el valor de estas remediciones post fuego, permitiendo el análisis de la trayectoria post-fuego del ecosistema en relación tanto con los impactos inmediatos post fuego como de las condiciones previas pre-fuego.

Background

Historical and contemporary wildfire activity and patterns within the mesic, highly productive forests of the western Cascades in Oregon and Washington are strongly driven by mean and interannual climate variability, where fuel moisture is the major factor limiting fire spread (Agee 1993; Reilly et al. 2021). In early September of 2020, extreme forest fuel aridity coincided with human- and lightning- caused ignitions and strong easterly winds, burning over 300,000 hectares of forested lands distributed across a range of land ownerships and contemporary forest management legacies. These six synchronous megafire events (i.e., > 10,000 ha burned; Linley et al. 2022), referred to hereafter collectively as the Labor Day 2020 Fires, exploded over a 2-day period driven by intense easterly winds and extremely dry conditions (Abatzoglou et al. 2021). Rapid crown fire spread and extreme fire intensities burned thousands of hectares, creating large patches of high severity outcomes (Reilly et al. 2022). Due to their extent and severity, these megafires will have significant, long-lasting impacts on ecosystems, landowners, and land-users in the western Cascades (Fig. 1).

While studies have summarized burn severity patterns and/or modeled drivers of fire effects at broad-scale across the Labor Day 2020 Fires via remote sensing (Evers et al. 2022; Reilly et al. 2022), detailed field observations of post-fire tree survival and the status of tree crowns and soils are needed to better understand the impact of these fires on forest ecosystems. Such information is essential for estimating these fires' effects on forest carbon trajectories, how and the extent to which pre-fire forest structure drives fire effects, standing and downed wood legacies in the post-fire forest, changes in soil organic matter, needs and opportunities for post-fire management (e.g., salvage logging and rehabilitation), and to validate and refine empirical models, remote sensing products, and indices that predict fire effects.

While others have collected field-based post-fire forest data to support a variety of research objectives, few

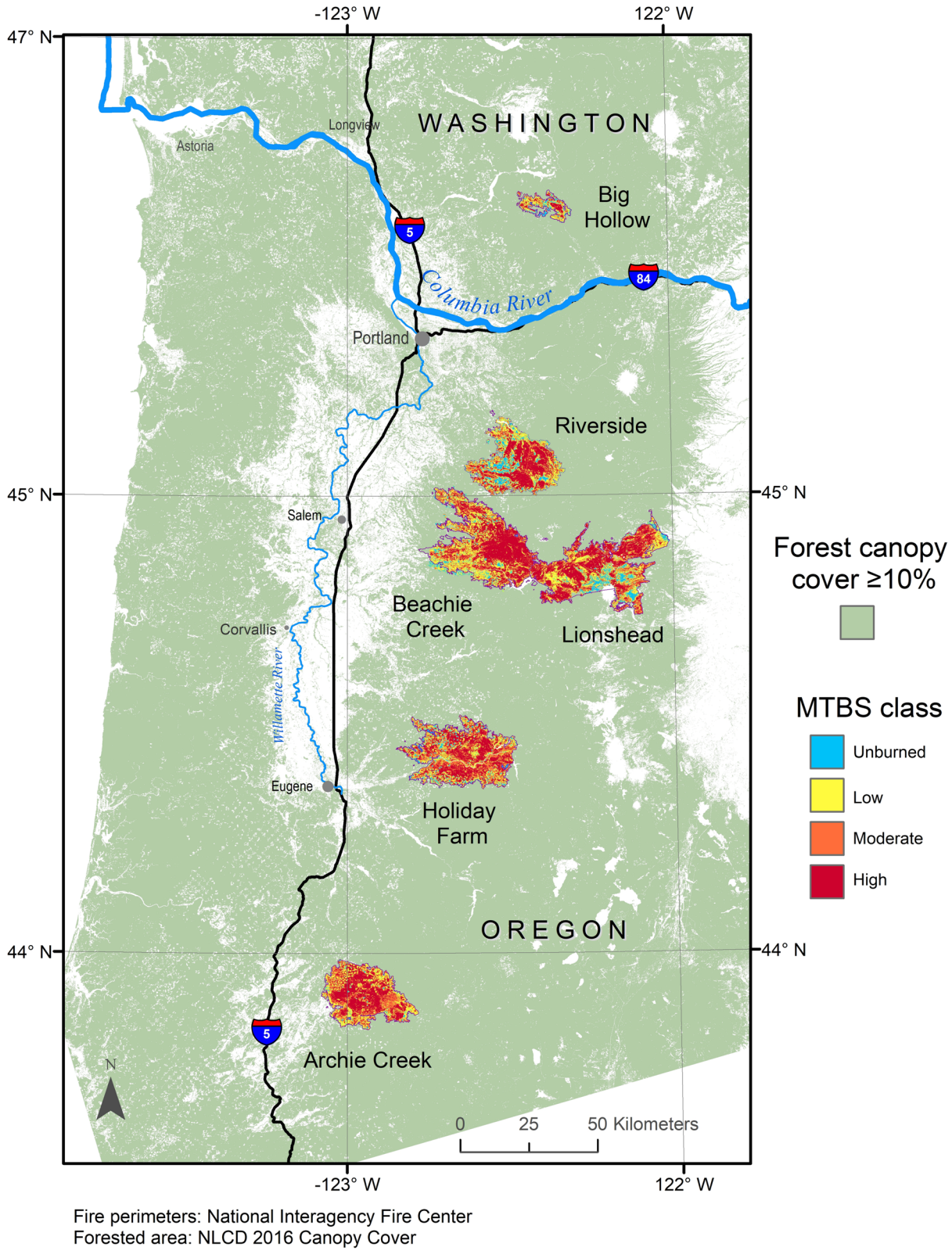

Fig. 1 The six fire events that comprise "the 2020 Labor Day fires" in Oregon and southwest Washington, attributed by remotely sensed Monitoring Trends in Burn Severity (MTBS) burn severity class. Light green shading indicates forested area with at least 10% canopy cover as reported by the National Land Cover Dataset (NLCD)

have leveraged pre- and post-fire data owing to a dearth of extant plots sampled under a consistent protocol (researchers lack foreknowledge of future fire footprints) or the high costs and exceptional logistical challenges associated with the timely remeasurement of plots. When pre-fire data are absent, pre-fire forest characteristics are sometimes "reconstructed" by inference from post-fire observations and fire age, injecting unknown degrees of imprecision and uncertainty into a field "observed" dataset before analysis even begins. The USDA Forest Service's Forest Inventory and Analysis (FIA) program collects a spatially balanced and statistically representative sample of forests in the USA via an extensive network of permanent, field-measured inventory plots. Recurring field measures from FIA plots provide a detailed and spatially and temporally consistent source of data valuable for characterizing forest structure and understory attributes. In the western US over the past two decades, a measurement cycle consists of ten annual panels, each comprising 10% of the plots—hence its name: annual inventory. A Fire Effects and Recovery Survey (FERS) protocol has been developed, implemented, and refined to augment the standard FIA inventory protocol with a rapid (typically within 1-year post-fire) off-cycle remeasurement visit. Post-fire remeasurements collect all the standard FIA measurements plus data needed to evaluate the effects of fire on tree crowns and ground surface substrates, enabling estimation of fire impacts across forest classifications of interest such as forest type, age and structure class, and landowner group. Intermittently implemented in years with large area burned that coincided with availability of funds to collect data, the protocol was until now implemented almost exclusively on federal lands and never in the "westside" forest region of Oregon and Washington where large fires have been rare since before the annual inventory began circa 2001. A coproduction effort to exploit the unique learning opportunity these fires afforded and pooled resources among the Oregon Department of Forestry, Bureau of Land Management, and the USDA Forest Service's PNW Region and PNW Research Station enabled collection of FERS data from 236 forested FIA plots, across all ownerships, in the western Cascades within the perimeters of six Labor Day 2020 fire events by the end of 2021.

Under projected increases in fire activity this century within the western Cascades (Halofsky et al. 2018a, 2020), uncertainty persists as to whether high severity (i.e., > 75% overstory tree mortality) megafire events will become more frequent (e.g., 2022 Cedar Creek Fire; > 50,000 ha) and, further, if and how mesic westside forests can be managed to enhance fire resistance under moderate to severe fire weather (Halofsky et al. 2018b). Owing to a low incidence of large wildfires in westside forests over the last half-century, empirical data have been too limited to test hypotheses linking forest structure to fire severity, and especially under the kind of extreme fuel aridity and east winds that drove infrequent high-severity megafires in the historical record (e.g., 1902 Yacolt Fire), and which comprise a critical share of the historical western Cascades fire regime (Agee 1993; Reilly et al. 2021). Thus, pre- and post-fire FIA data collected from the Labor Day 2020 Fires present a unique and invaluable dataset for exploring a variety of questions and testing hypotheses related to fire effects in western Cascades forests.

This paper demonstrates the potential of FERS data to address fundamental questions in forest fire ecology and to assess consistency of the remote sensing representations of fire severity that are so often relied upon in ecological assessments of fire effects. We developed and implemented repeatable procedures for processing FIA pre- and FERS post-fire data into stand-level fire effect responses in the form of post-fire indices that characterize the short-term transformation of these forests by fire from multiple, policy- and management-relevant perspectives. These indices classify the post-fire forest landscape in a way that may explain differences in post-fire early seral legacies and implied management needs, suggest implications for forest carbon dynamics, and provide a basis for contrasting outcomes generated by alternative pre-fire forest stand structures. We summarize (1) tree survival (and related carbon implications), (2) effects on forest canopy via tree crown consumption and scorch, and (3) effects on soil organic matter and integrity. To account for and understand the effect of wind speed on observed fire effects across plots (i.e., the primary driver of fire spread, intensity, and severity of effects), we linked spatially explicit, modeled hourly mean wind speed data with custom interpolations of fire progression maps to estimate wind speed when the fire front first contacted each FIA plot. The integration of these data enables this paper to address four policy-relevant research questions for the 2020 westside fires:

1. How do fire effects (tree survival, crowns, and soils) vary by fire perimeter, ownership, forest age & structure class, and by estimated windspeed?
2. How much tree biomass has been converted from live to dead due to fire, by ownership and stand age class?
3. On how much forest area did post-fire salvage logging occur during the first-year post-fire and how much tree biomass was harvested?
4. How closely do remotely sensed burn severity product classifications track field observed fire effects?

Methods

Study area

We analyzed pre- and post-fire forest survey data from 236 forested FIA plots distributed across six distinct 2020 Labor Day Fires that burned in the western Cascades mountains from central Oregon north to SW Washington (Fig. 1). A mesic Mediterranean climate with warm, dry summers and cool, wet winters prevails here, with increases in annual precipitation and decreases in annual temperature following both a west-to-east elevational gradient and a south-to-north latitudinal gradient. Soils in these landscapes are primarily well-drained, ashy sandy loam andisols (USDA 2022). A mesic climate and limited fire frequency and extent has produced high stand density and nearly continuous canopy cover, with few large (> 5 ha) open patches distributed across the landscape that do not result from regeneration harvesting. Most low elevation forests on the western edge are privately owned, managed predominantly for timber production, and have a tree canopy composed overwhelmingly of Douglas-fir (*Pseudotsuga menziesii*). The mid-to-high elevation forests farther east are largely administered by the USDA Forest Service as national forests or by the Bureau of Land Management as BLM district forests. Habitat, ecosystem services, and recreation are prominent management objectives for both agencies; however, there is greater timber production emphasis on BLM lands. Many high-elevation forests near the Cascade Crest are within designated wilderness. At mid-elevations, tree species composition is commonly dominated by western hemlock (*Tsuga heterophylla*) and/or Douglas-fir and at high-elevations by Pacific silver fir (*Abies amabilis*) and/or mountain hemlock (*Tsuga mertensiana*) (Franklin and Dyrness 1973). Except for moderately fire-resistant Douglas-fir, most species are shade-tolerant and fire-sensitive (i.e., with thin bark and canopies approaching the ground; Agee 1993). Pre-fire species composition (proportion of live tree volume) observed in FIA plots across fires was largely dominated by Douglas-fir (~ 71%) followed by western hemlock (~ 12%); western hemlock abundance increased with latitude (~ 7% in Archie Creek fire to ~ 25% in Big Hollow fire; Table S1). See Table 1 for summary statistics on the areal distribution of forest size and age classes by ownership.

Table 1 Area (in thousand hectares) and percent (in parentheses) of forest area by owner group in each pre-fire stand size and age class within the six 2020 Labor Day fires. Percentages are for each owner and structure combination totaled by column within class type

Forest structure	NFS	BLM	State	Private	All
Size class (cm)[a]					
< 25	20 (18%)	4 (11%)	4 (36%)	44 (45%)	72 (28%)
25–53	51 (46%)	15 (41%)	2 (17%)	53 (53%)	121 (47%)
> 53	40 (36%)	18 (48%)	5 (47%)	2 (2%)	65 (25%)
Age class (years)					
0–20	6 (5%)	0 (0%)	3 (27%)	37 (29%)	46 (15%)
21–60	37 (32%)	17 (40%)	3 (27%)	83 (64%)	140 (47%)
61–120	34 (30%)	12 (28%)	3 (27%)	3 (2%)	52 (18%)
121–150	7 (6%)	8 (19%)	2 (18%)	0 (0%)	17 (6%)
> 150	30 (26%)	6 (14%)	0 (0%)	0 (0%)	36 (12%)
All age classes	114	43	11	129	297

[a] Stand size classes: < 25 cm (< 10 in), 25–53 cm (10–20 in), and > 53 cm (> 20 in) diameter

Data acquisition and processing

Description of pre- and post-fire field data

FIA is a nationally consistent forest inventory and monitoring program based on permanent plots designed to be maintained and remeasured in perpetuity, with core and core-optional protocols adopted by some regions; for example, down wood and understory vegetation core-optional protocols have been followed in CA, OR, and WA in the PNW region since implementation of the annual inventory system. These protocols are defined and documented in both database documentation (FIADB Users Guide; Burrill et al. 2021) and regional field guides (USDA Forest Service PNW Research Station FIA 2022), from database use and field implementation perspectives, respectively.

The plot "footprint" is a mapped design consisting of a sampled area formed by a quartet of 7.3 m (24 ft) radius subplots for sampling trees larger than 12.7 cm (5 in) diameter at breast height (DBH), each containing a 2.1 m (6.8 ft) radius microplot to sample small trees and coincident with a concentric, 18 m (58.9 ft) radius macroplot on which the largest trees (those over 76.2 cm [30 in] in diameter) are sampled. The quartet is arranged as three satellite subplots arrayed symmetrically around a central subplot at 36.6 m (120ft) distance and 120-degree intervals. This sampled area is partitioned into separate "conditions" when delineation-qualifying differences (e.g., in owner group, forested status, reserve status, forest type, stand size class, tree density class) exist and minimum condition size and shape criteria are satisfied. Site attributes such as slope, site quality, stand age, forest type, and landowner group are defined and collected at the condition level, and each condition can be thought of as a "stand," providing a comparatively homogeneous sampling unit on which analysis can rely. Conditions occupying less than 20% of a plot's area were excluded from all summaries except the carbon analysis in this paper, with the area they represent reallocated proportionally

to the rest of the conditions. Small conditions, sometimes termed slivers, commonly increase the risk of introducing artifacts and noise when calculating tree survival (e.g., at the extreme, a condition containing one tree can only produce a tree survival proportion of 0 or 1) and have such low tree tally that the information represented by those trees does not adequately represent a forest stand, or in the worst case, the forested condition (identified as such based on the presence of trees on portions of the condition that extend outside the plot footprint) may contain no trees at all, making it impossible to calculate stand characteristics that we might want to test in relation to survival, for example, canopy bulk density.

All trees on each forested condition are assessed for status (live or dead), measured for diameter, assessed for height, crown ratio, defect and disease, and monumented with metal tags and diameter nails at each visit, with all trees sampled on 2nd and subsequent (i.e., remeasurement) visits having their data reconciled in the field against measurements from the previous on-panel visit to detect, prevent, and resolve measurement errors and to enable precise characterization of growth, removals and mortality.

Calculation of post-fire tree survival

Fire effects on tree vegetation at stand, as opposed to individual, scale can be expressed in terms of observed mortality or survival rates of tree count on a plot, or alternatively, trees, basal area, wood volume, or wood biomass per unit area (each of which can be obtained via expansion of the per plot values and in the case of volume and biomass, application of allometric equations to tree species, diameter and height). In this paper, we chose to report on stand level survival rates for wood biomass per ha, i.e., wood in live trees that remain live 1-year post-fire as a proportion of wood in live trees pre-fire for several reasons. What the fire leaves behind in surviving trees was slightly more resonant as a fire outcome metric than mortality with forest managers, analysts, and policy actors we consulted. Biomass gives larger trees (which play a more significant role from some perspectives) more weight in the metric, though basal area and volume would also accomplish this. Relative biomass survival has implications that are important to both ecosystem function and policy relevant considerations such as retention of sequestered carbon in forested landscapes.

Tree survival was calculated from an FIA dataset of 9387 trees that were (1) on plots within the final fire perimeter, (2) alive before the fire, and (3) were observed to be alive, dead, or harvested post-fire. Trees that died from non-fire related causes or were harvested before the fire were excluded from this analysis. Trees were stratified into three size classes based on pre-fire diameter: ≤ 25.4 cm (≤ 10 in), 25.5–50.8 cm (10–20 in), and > 50.8 (> 20 in). For each FIA "condition" (a full or partial FIA plot), tree survival proportion (TSP) for each tree size class, and for all size classes combined, was calculated as the ratio of total above-ground live tree biomass (kg/ha), measured before the fire, in that tree size class in trees that remained alive post-fire to the total live biomass in that tree size class pre-fire. Biomass per tree was calculated using standard FIA methods, which rely on species specific allometric equations for bole, bark, and branches (Woodall et al 2011), and per hectare expansions, calculated with a coefficient that accounts for sampling scale (e.g., trees between 12.7 and 75.2 cm diameter were sampled on 0.067 ha plots and assigned an expander of 14.88, the inverse of plot size). The per ha biomass represented by each sample tree was then summed to the condition scale, and this sum divided by the proportion of the plot in the condition to achieve a sample-weight-adjusted per ha value. Salvage biomass was calculated for all trees that were harvested within a year or less following the fire. This included trees that may have initially survived the fire or died owing to non-fire causes; however, the salvage biomass consisted predominantly of fire-killed trees.

A post-fire index for crowns

While tree survival 1-year post-fire is an essential descriptor of what fire leaves behind on forested land relative to the forest that pre-dated fire's arrival, survival (or its complement, mortality) captures only some aspects important for understanding prospects for post-fire trajectories which, on the plots in this study, will be monitored for decades under the FIA inventory and monitoring system. While the fate of biomass is important for understanding site occupancy, future growth, reburn potential, protection from soil erosion, organic matter inputs to soil, and carbon emissions, so too are latent mortality, effects on crowns of trees that don't die and future inputs of litter to the forest floor, especially where few trees survive or where little soil organic matter remains.

We assigned a crown post-fire index (Crown PFI) to each FIA condition (stand), following a post-fire index for trees developed by Jain and Graham (2007), from observations of tree crowns at the FERS post-fire visit, to address some of these ecologically important facets of the post-fire environment. To calculate Crown PFI, we considered only trees that were alive before the fire and that either remained alive or were killed as a direct consequence of the fire ($n = 6771$). All conditions containing trees coded as salvage were excluded from the analysis of crown PFI ($n = 28$), regardless of whether the trees were fire-killed before salvage, because crown status

could not be observed on trees removed before inventory crews arrived. At the post-fire visit, crews recorded the percentages of the pre-fire compacted crown length, computed as the product of pre-fire compacted crown ratio and pre-fire tree length (length = height for a tree that has no lean), in up to three categories that sum to 100%. A field guide (USDA Forest Service PNW Research Station FIA 2021) describes these three categories as foliage that is unburned (green), scorched (branches with attached foliage that has transitioned from green to brown, red, orange, yellow or black), or consumed (blackened branches to which foliage had been attached that, by the time of observation, were all but devoid of foliage, with perhaps a few blackened remnants or with branches and foliage completely combusted, i.e., no longer there to be observed). We used the key in Table 2 to assign the best-fitting Crown PFI class (green, mixed green, mixed brown, brown, transition, or black) to each FIA condition (stand).

Crown PFI is reported to be flexible and applicable to any subset of trees in a stand. To learn how it might vary by tree size, we derived three variations of Crown PFI, one for each of three overlapping tree subsets with alternative minimum tree diameters:> 2.25 cm (>1 in), >; 12.7 cm (> 5 in), and > 22.5 cm (> 10 in).

A post-fire index for soils

We assigned a post-fire soil index (Soil PFI) based on classifications of ocular estimates of organic matter cover (OMC; ≥ 85%, > 40 to < 85%, > 0 to < 40%, or 0%) and mineral soil char class plurality (unburned, light, moderate, or deep) collected on up to 4 microplots (13.44 m^2 each) in forested conditions at the post-fire field visit, following Jain et al. (2012). See Table S2 for the classification key. Analogous to crown PFI, soil PFI offers a framework for characterizing differences in the post-fire environment that may foreshadow different stand trajectories (e.g., erosion potential, soil fertility and moisture-holding capacity) and the vegetation likely to colonize the site. Conditions where salvage harvest occurred were excluded from the analysis because the movement of harvesting equipment would have likely caused changes in organic matter cover and exposed mineral soil, leaving 186 analyzable conditions.

Estimation of wind speed at fire arrival

The expectation that wind would be a very important driver of fire effects motivated concerted effort to account for wind speed as precisely as practicable for this analysis. Initial attempts at analysis using daily weather averages per fire yielded unsatisfying results. Though most of the fire extent in each of the 2020 Labor Day Fires burned within 2–3 days under strong winds, there was considerable variability in wind speed, and direction, over space and time during those few days of active fire spread, making it important to link each inventory plot to the weather data representing conditions at the time fire encountered that plot. This requirement implied two difficult challenges: (1) estimating the hour at which each plot first received fire and (2) estimating the wind speed and other relevant fire weather variables (such as temperature and relative humidity) that could represent conditions at the plot location. The first challenge should not be underestimated. We attempted to use several publicly available satellite-based sources to identify that hour and obtained wildly divergent results owing to high spatial resolution but low refresh frequency of one source and high refresh frequency but very coarse spatial resolution of another. Briefly summarized below is the approach that proved most successful (Klock et al. 2023).

For large fire events in the USA, the Forest Service's National Infrared Operations (NIROPS) unit provides

Table 2 Key for assigning stand-level crown post-fire index (PFI) based on distributions of trees per acre (tally trees weighted by inverse of plot size) by crown status

Post-fire characteristics of the condition			Crown PFI class
1:	Residual green (unburned) crowns present—"Alive" superclass		
	1a	All trees that were live immediately pre-fire have ≥ 70% residual green (unburned) crown	Green
	2b	At least half of trees have at least 30% of their crown length green (unburned), and none of their crowns contain black (consumed), though some are brown (scorched)	Mixed green
	3c	Some (potentially less than half) of the trees contain some green (unburned) in their crowns, some contain brown (scorched), and some may contain black (consumed)	Mixed brown
2:	Residual green (unburned) crowns absent—"Dead" superclass		
	2a	All trees have at least 90% of their crown length brown (scorched)	Brown
	2b	There is a mixture of trees with brown (scorched) crown, both brown and black (consumed) crown and only black crowns	Transition
	2c	All trees have at least 90% of their crown length black (burned) or consumed	Black

spatial data on fire extent derived from visible/near infrared (IR) sensors mounted on aircraft conducting fire survey missions that accurately represent, at a scale of meters, location of the fire front at the time of the overflight. We retrieved these IR fire perimeters from the National Interagency Fire Center (NIFC) Operational Data Archive 2020 (https://data-nifc.opendata.arcgis.com/). Unfortunately, processing of IR data to produce fire perimeters is sometimes delayed by several days, and these flights occur at unpredictable, sometimes multi-day intervals that are likely dependent on fire conditions, weather, and available resources. Anomalies, such as perimeters that contract in one or more segments from one day to the next, widely varying perimeter intervals and an abundance of duplicate records present challenges to using this information for our intended purpose. Duplicates were filtered and cross-checked against supplemental data logs to obtain accurate acquisition times.

The NIFC fire perimeters were selected for processing if they fell within the final fire perimeter and the time of interest for each incident (generally September 7–11, 2020). Because the date and time stamps reported for each perimeter proved less than fully reliable, we refined them by integrating information from fire data logs, fire size growth (acres), alignment with IR points or spot fire location data, and Google Earth KMZ files downloaded from the NIFC Incident Specific Data website (https://ftp.wildfire.gov/public/incident_specific_data).

To obtain a temporal resolution on plot-fire encounters finer than the sometimes 24 + hour interval between NIFC generated time stamp perimeters, we developed a process for estimating the position of additional, approximate perimeters interpolated between concentric mapped NIFC perimeters guided by ancillary information in a geographic information system (GIS). To inform the location of these additional "perimeters," we relied on output from the Weather Research Forecasting (WRF) simulation model formulated for the Pacific Northwest region for September 2020; parameterization is described in detail by Mass et al. (2021). This model characterizes mean wind speed and direction at 10 m above the land surface and temperature and relative humidity at 2 m and generates output as a three-dimensional NetCDF raster file format, where each 1.3 × 2.0 km grid cell has a location, time (hourly resolution), and variable value dimension.

We partitioned the time interval spanning each concentric adjacent NIFC perimeter pair into 4 equal-length analysis time periods (APs). We calculated mean wind speed and direction for each AP for the WRF data covering the time defined by that AP, then visualized that wind information via iterative, hourly color ramps in the heads-up digitizing map background to guide spatial placement of three, approximate, interpolated perimeters that partitioned the fire growth represented by the AP into four spatially defined quartiles. This process was repeated for each concentric adjacent genuine NIFC perimeter pair as needed to partition the entire fire progression period into toroidal AP-quartile polygons attributed with a time stamp midway between the time stamps of the quartile boundaries that formed them. Overlaying exact FIA plot coordinates on time stamp attributed polygons derived for all six fires enabled assignment of an approximate time stamp representing arrival time of the fire to each plot. Finally, weather attributes (wind speed and direction, temperature, and relative humidity) were assigned to each plot via overlay with the WRF grid closest in time to the plot's fire arrival time.

Statistical analysis of wind speed effect

Given the widely held hypothesis that these fire events were primarily wind-driven, we tested for a threshold effect by computing all pairwise dissimilarities (distances) between observations based on a Euclidian metric with determination of the medoid by a robust partitioning method (PAM). The optimal number of clusters was selected by evaluating the average silhouette width and the variance explained by the first two principal components with the R package "cluster" (Maechler et al. 2021). The cluster analysis identified two relatively homogenous clusters, one on either side of 2.25 m/s (5 mph); thus, data summaries were classified into two mean wind speed groups, referred to as light (< 2.25 m/s) and moderate to strong (> 2.25 m/s) in the remainder of this paper. Mean wind speed averages gusts and lulls over time, such that gusts much higher than the mean wind speed may have occurred. For example, 4–9 m/s gusts might be observed under a mean wind speed of 2.25 m/s and > 16 m/s gusts observed under a mean wind speed of 9 m/s.

A series of parametric and non-parametric approaches were utilized to understand the association between the post-fire responses (e.g., tree survival, crown PFI, and soil PFI) and weather, land ownership, fire identity, and forest structure attributes. All continuous responses were evaluated for meeting the assumptions of normality (if applicable), and to reduce experiment wise error rates (type I error, falsely rejecting the NULL), we adopted a more stringent level of significance for all pairwise comparisons with Bonferroni correction (Bland and Altman 1995). We used an alpha level of 0.05 for all statistical tests and the analysis was conducted in the programming language R (R Core Team 2022).

Live tree carbon effects

We generated a preliminary statistical estimate of fire outcomes for the carbon stored in live trees via FIA's

stratified estimation tools (Bechtold and Patterson 2005), using a stratification customized to the fire footprints with non-sampled plots assumed to be missing at random, to expand live tree carbon outcomes on FIA sample plots to the area within the 2020 Labor Day fires (e.g., enabling comparisons of carbon outcomes by owner group and pre-fire forest conditions). These estimation tools also support ratio of means estimators such as amount of live tree carbon that moves from live trees to dead wood and atmospheric pools per hectare, facilitating policy-relevant analysis and comparisons of outcomes across forest structures and ownerships with different areal extents. These estimates consider stand-level pre-fire live tree carbon to be the calculated woody carbon content based on the most recent pre-fire tree measurements in trees attributed by field crews at the post-fire visit as having been live immediately preceding the fire, summed, with tree expansion weights assigned based on the plot size on which each tree is sampled, over all such trees on the forested FIA condition. Trees with a post-fire status of dead or harvested and utilized and for which fire is assigned as the cause of death are considered, in the short term, to have left the live tree pool for one or more of the following pools: unutilized dead wood, harvested wood products, or atmospheric emissions. This accounting understates losses from the live tree pool because ingrowth trees (which are not accounted for in the pre-fire inventory data and which, owing to their smaller size, are more likely to die by fire) and live tree growth since the previous measurement would increase live tree losses if we were able to account for them. It also does not address the immediate carbon emissions that result from combustion of standing and down dead wood and forest floor components such as duff and litter, which can be considerable.

Remotely sensed burn severity products

To compare the agreement between two remotely sensed burn severity product classifications commonly utilized by managers and observed fire effects on FIA plots, we conducted a spatial overlay to extract classified product values at each FIA plot location. Specifically, we extracted values from the Burned Area Emergency Response – Soil Burn Severity (BAER-SBS) and Monitoring Trends in Burn Severity – Thematic Class (MTBS-TC) products. Given the spatial resolution of BAER-SBS and MTBS-TC products (30 m) is finer than the FIA plot footprint (i.e., many pixels are nested within the plot footprint), we used a majority filter with an 8-pixel kernel (0.81 ha footprint) to represent classified burn severity values at the FIA plot level.

The BAER-SBS product is commonly used to inform post-fire assessments of soils and understory vegetation conditions over space while the MTBS-TC product is commonly used to inform assessments of fire-caused vegetation and tree mortality patterns over space. Both products are derived from the differenced normalized burn ratio (dNBR) spectral index using systematic and subjective methods. Given each product's common usage by managers, we compared BAER-SBS classifications to plot-derived Soil PFI classifications and MTBS-TC classifications to plot-derived tree biomass mortality proportions.

The BAER-SBS and MTBS-TC products are classified as discrete thresholds of dNBR into unburned (1), low (2), moderate (3), and high (4) burn severity categories. Following descriptions written by the agency that hosts these products (USGS 2022), fire effects associated with each burn severity category can be generalized as:

(1) Unburned or when fire effects are recognizable on less than 5% of the site. The class may also include areas that recover very quickly following a light, surface fire occurring under dense forest canopies that were unaffected by fire.
(2) Low burn severity includes substrates and litter that may be partially to completely consumed; duff, down wood and exposed mineral soils typically show some change. Vegetation < 1 m and shrubs or trees 1–5 m may show significant scorch, char or consumption, and vegetation mortality may be high. Intermediate and large overstory trees may exhibit up to 25% mortality with crown consumption or scorch and char height typically less than 3 m.
(3) Moderate burn severity represents conditions that are transitional in magnitude and/or uniformity between the characteristics of low and high burn severity. A large proportion of ground cover may be consumed, but generally not all of it.
(4) High burn severity represents areas where substrates and litter are totally consumed, duff is almost entirely consumed, medium and heavy down wood is at least partially consumed and deeply charred; overstory trees exhibit > 75% mortality, crown consumption usually 100% and significant branch loss at the highest crown heights.

Results

Post-fire tree survival

Tree survival proportion (defined here as the proportion of pre-fire live tree biomass found in trees that remain alive 1-year post-fire; TSP) varied greatly among stands, with mean wind speed at the estimated time of a stand's encounter by the fire front acting as a strong driver across the range of tree size classes (Fig. 2).

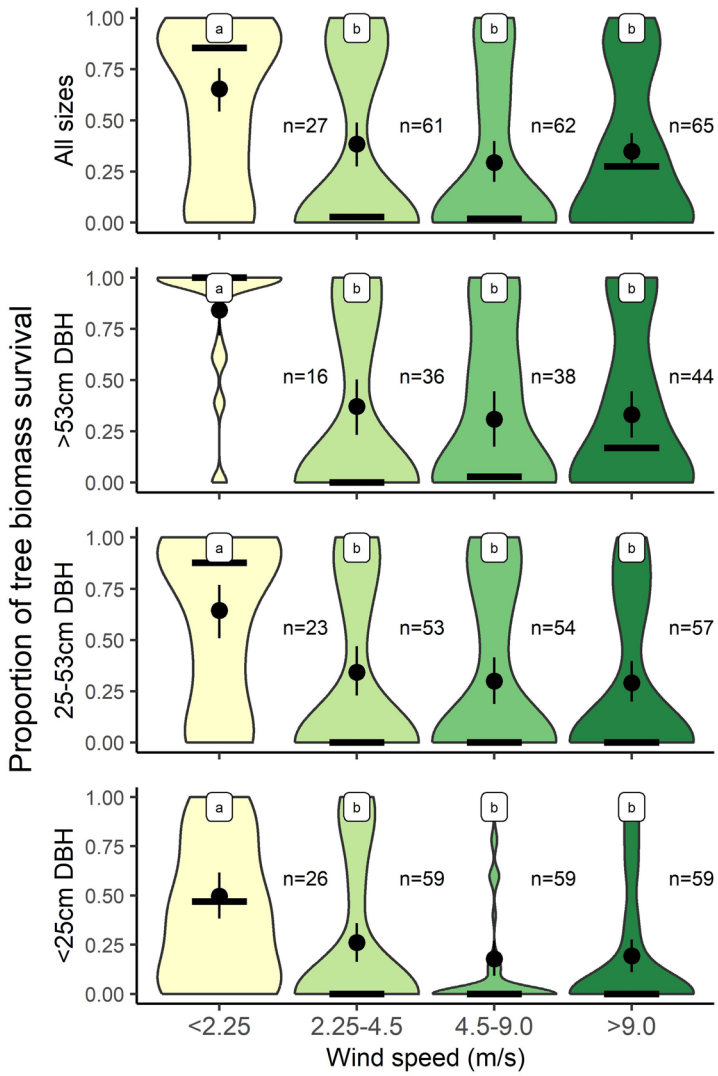

Fig. 2 Distribution of the proportion of surviving tree biomass (post-fire live biomass/pre-fire live biomass) by tree diameter class and modeled plot-local wind speed class at fire arrival. Metrics represented are means (black circles), medians (black horizonal bars), 95% confidence intervals (black vertical line), and "*n*" which references the number of forested conditions on which trees were present in the associated tree diameter class and wind speed class. Statistical differences are indicated by letter assignments among wind speed groupings for a tree diameter class (Wilcoxon rank sum test; $\alpha = 0.05$)

Pairwise comparisons (Wilcoxon rank sum test) among wind speed groupings revealed a statistically significant 2.25 m/s (5 mph) threshold effect on TSP. Light winds (< 2.25 m/s) were associated with substantially greater mean and median TSP for all tree sizes (0.65–0.80 vs 0–0.40). Under light winds, trees in medium (> 25.4 cm; > 10 in DBH) and large (> 53.3 cm; > 21 in DBH) size classes were more likely to survive; large trees exhibited a particularly high survival rate (mean > 0.80), and there were very few cases of low survival. There were no significant differences in TSP across tree size classes among wind speed groupings greater than 2.25 m/s, though median TSP was slightly greater for large trees and for all tree size classes combined under extreme winds (> 9.0 m/s).

There are indications of a potential latitudinal effect on TSP for all tree size classes, with mean and median TSP increasing with latitude of fire perimeter centroids. In the northernmost fires (Riverside and Big Hollow), TSP was significantly greater than in the southernmost fires for some tree size classes (Fig. 3). Winds were lighter in the Archie Creek and Big Hollow fires, on

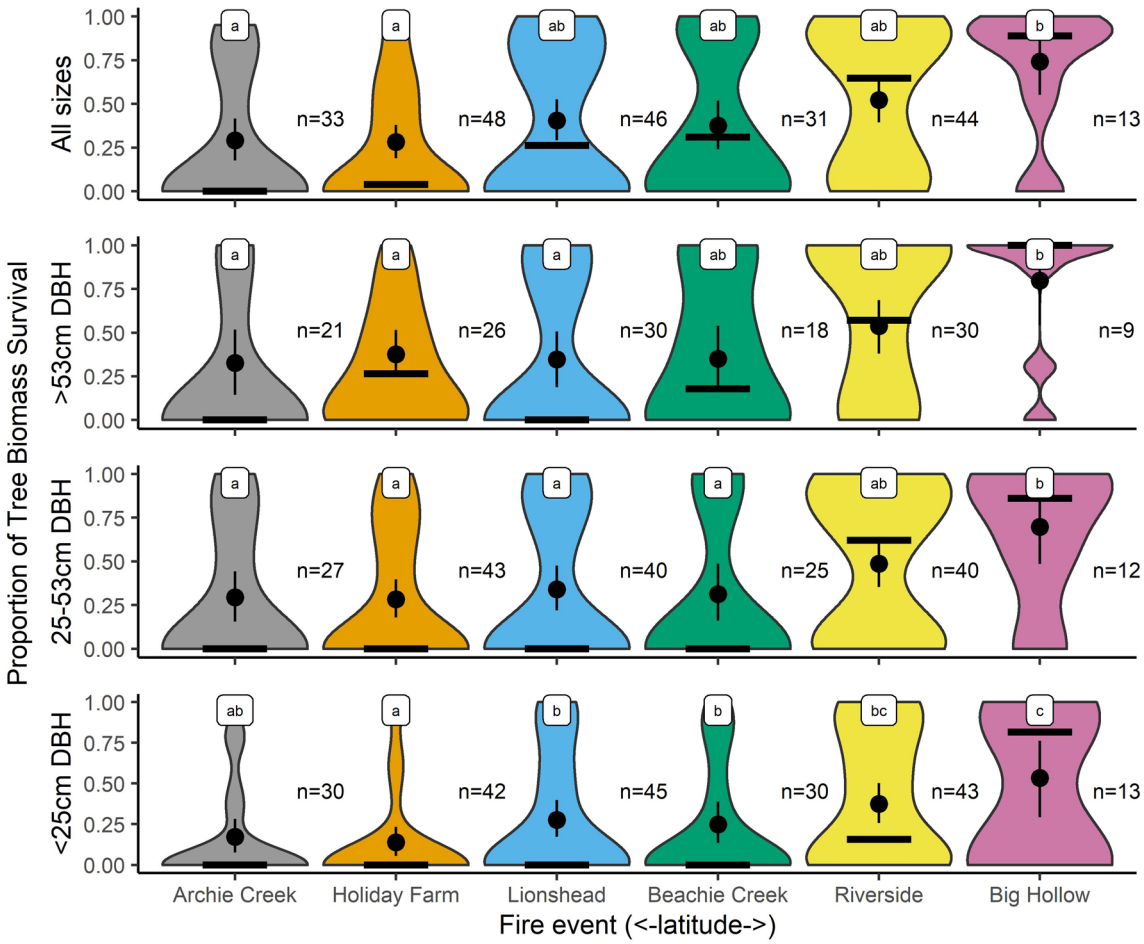

Fig. 3 Distribution of the proportion of surviving tree biomass (post-fire live biomass/pre-fire live biomass) by fire event (with increasing latitude left to right) and tree diameter class. Metrics represented are means (black circles), medians (black horizonal bars), 95% confidence intervals (black vertical line), and "*n*" which references the number of forested conditions on which trees were present in the associated fire event and tree diameter class. Statistical differences are indicated by letter assignments among groups in each tree diameter class (Wilcoxon rank sum test; $\alpha = 0.05$)

average, and relative humidity was greatest in the Big Hollow fire (Table S3).

Tree survival proportion differed among ownership classes when winds were light and when wind was not considered, but differences under moderate-strong winds were not significant (Fig. 4). Under light winds and all wind classes combined, survival was significantly greater in national forests than in private forests. By reducing survival, often dramatically, and by increasing variation in outcomes, wind speeds > 2.25 m/s rendered differences insignificant among ownerships.

When all wind speeds were considered, TSP was significantly greater in stands 60–120 years old than in stands > 120 years old (Fig. 5); differences in TSP among the five FIA-derived structure classes that combine broad diameter class and even vs uneven agedness were mostly not significant (Figure S1). Considering only light winds (< 2.25 m/s), TSP was significantly greater in stands 60–120 years old than in stands 0–60 years old and in even-aged stands dominated by 23–51 cm (9–20 in) DBH trees than in even-aged stands dominated by < 23 cm (9 in) DBH trees. Under moderate to strong winds, TSP was significantly greater in stands 60–120 years old than in stands older than 120 years, and structure class was not a significant driver of survival. Generally, mean and median TSP were greatest in 60- to 120-year-old stands, and even-aged stands dominated by 23–51 cm (9–20 in) DBH trees across all wind speed classes.

Post-fire crown and soil effects

The distributions of Crown PFI were robust to assumptions about minimum tree size choice for computing the index; no significant differences were detected among the three thresholds we posited for implementing this index. Given that the FIA plot size on which trees < 12.7 cm (5 in) diameter are sampled is less than a tenth the size on

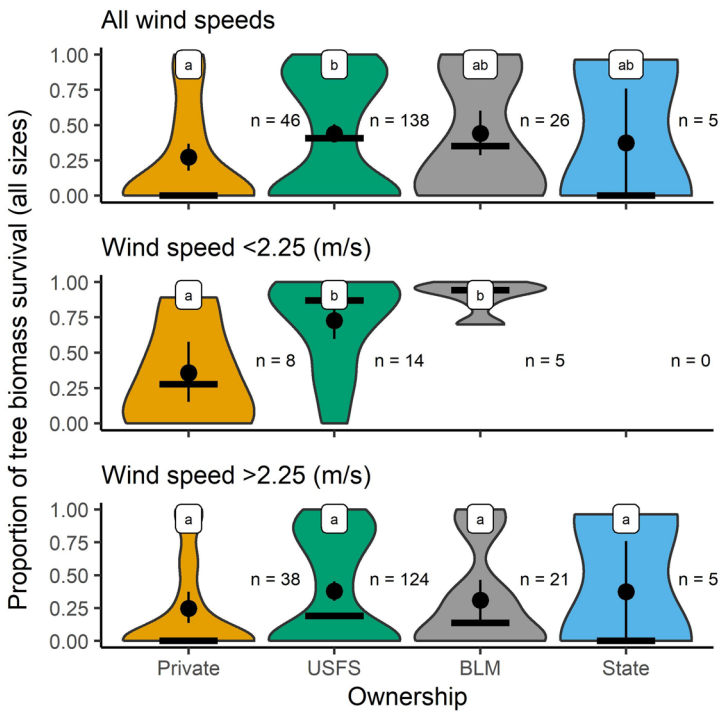

Fig. 4 Distribution of the proportion of surviving tree biomass (post-fire live biomass/pre-fire live biomass) by forest owner group and modeled plot-local wind speed class at fire arrival. Metrics represented are means (black circles), medians (black horizonal bars), 95% confidence intervals (black vertical line), and "*n*" which references the number of forested conditions on which trees were present in the forest owner group and wind speed class. Statistical differences are indicated by letter assignments among groups in each wind speed class (Wilcoxon rank sum test; $\alpha = 0.05$)

which trees ≥ 12.7 cm are sampled (such that outcomes could differ by tree size in a spatially heterogeneous fire environment that happens to spare or deeply impact the sapling plot), we present stand level Crown PFI outcomes calculated using only trees larger than > 12.7 cm (5 in).

Under light winds, 97% of the forest area that was not salvage logged was classified as having a Crown PFI of green, mixed green or mixed brown, with the remaining percent classified as transition—an outcome that occurred only on the Holiday Farm fire (Fig. 6). However, the nearly 9% of the forest area burned under light winds that experienced salvage harvest within ~ 12 months of the fire would likely have been assigned one of the higher Crown PFI classes had salvage before the post-fire visit not prevented assessment of crown outcomes. Forests encountered by fire when winds were moderate to strong experienced a very different outcome—Crown PFI for 46% of that area across all fires was classed as brown, transition, or black (i.e., virtually no unburned crown remained). Assuming that salvage was prioritized where mortality was greatest (and brown, transition or black Crown PFIs were most likely), up to 50% of area burned under moderate-strong winds was essentially devoid of live canopy post-fire.

Post-fire, most forest area was observed to have between > 0% to < 40% organic matter cover (OMC) and light (60% of area) or moderate (13.8% of area) charring of mineral soil (Fig. 7). Unlike Crown PFI, the distribution of Soil PFI was similar under light and moderate to strong winds, although 0% OMC was only observed under moderate to strong winds (these classes collectively represent only 5.3% of the forest area, however). Given that roughly 98% of the forest area had OMC ≥ 85% pre-fire on national forests (the only ownership on which ground cover was consistently evaluated pre-fire), the distribution of Soil PFI post-fire indicates major losses of OMC.

Initial outcomes for live tree carbon

National forests within these fires contained the largest live tree carbon pools both before (53.8 MMT CO_2e) and after (23.5 MMT CO_2e) the fires (Table 3; Table S4); this ownership actually increased its share of live tree carbon (from 48 to 55%) of stores on the forested lands within the fire perimeters. However, because national forests contained so much live tree carbon, there was more to be lost from the live pool. Live tree carbon survival was

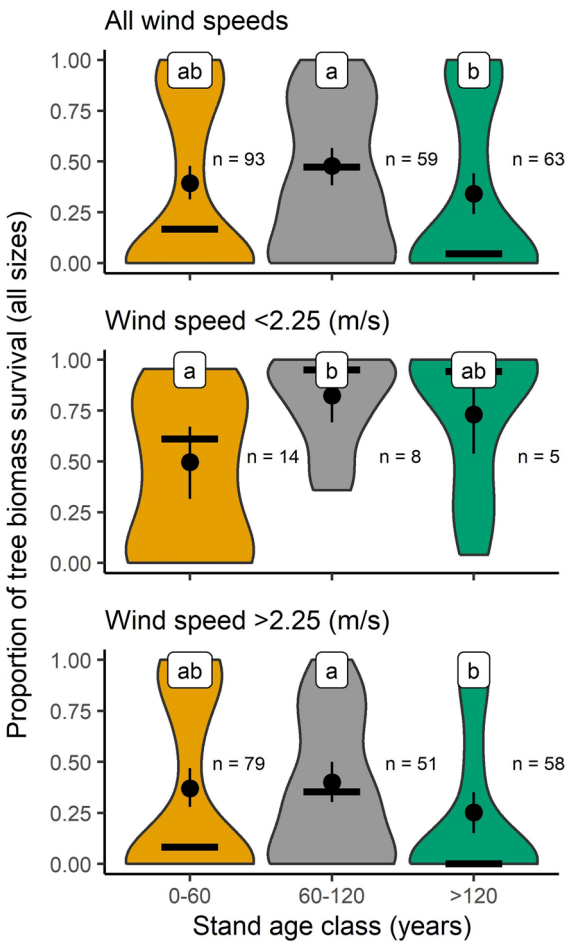

Fig. 5 Distribution of the proportion of surviving tree biomass (post-fire live biomass/pre-fire live biomass) by stand age class and modeled plot-local wind speed class at fire arrival. Metrics represented are means (black circles), medians (black horizonal bars), 95% confidence intervals (black vertical line), and "*n*" which references the number of forested conditions on which trees were present in the associated fire event and tree diameter class. Statistical differences are indicated by letter assignments among groups in each tree diameter class (Wilcoxon rank sum test; $\alpha = 0.05$)

only 37% in the oldest (> 120 years) stands that account for 43% of live tree carbon on national forests. The comparatively greater rates of tree survival in young (0–60) and mature (60–120) year-old stands elevated the live tree carbon survival rate across all age classes to 44% on national forests.

Private forests stored less live tree carbon pre-fire—not surprising given the preponderance of younger stands on that ownership and absence of stands older than 120 years; however, a large share of that carbon (73%) moved to other pools. Notably, most (56%) of the carbon in fire-killed trees on private lands had already been harvested in post-fire salvage operations by the time plots were visited 8–12 months following these fires. These operations undoubtedly transferred a significant share of woody carbon into harvested wood products, some of which will continue to sequester carbon for longer than the fire killed wood that remains in the forest. Salvage rates on national forests were comparatively miniscule (3% of fire killed tree carbon). Given a 0.09 median proportion of live tree carbon harvested on the 5733 ha of national forest where salvage occurred (vs. 0.97 on the 35,630 ha of private forests where salvaged occurred), salvaged wood on national forests was likely generated primarily by roadside safety operations, which may or may not have been utilized to the same extent. Salvage was rare on other ownerships.

Live tree carbon stores and outcomes expressed on a unit area basis show dramatic differences by ownership within these fires, with forests managed by the Bureau of Land Management holding the most carbon in live trees pre-fire and those that are privately owned holding less than a third as much, for all age classes combined (Table 3; Table S4). Conversions from live to dead are high for all ownerships in young stands. The mean live to dead conversion rates are high for all landowners except national forests for mature (60–120 years old) forests and for all public owners except national forests for forests older than 120 years. Forests managed by both Bureau of Land Management and Oregon Department of Forestry tend to be at lower elevations than those managed on National Forest land and thus might be subject to a shorter duration of exposure to east winds. Carbon representing 72 metric tons CO_2e per ha in fire-killed trees was removed via salvage on private lands in young forests; it was much lower elsewhere, and for some combinations of stand age and ownership, there was no salvage recorded on FIA plots in the first-year post-fire.

Comparisons to remotely sensed burn severity products

Although BAER-SBS burn severity showed a degree of correspondence with organic matter cover (OMC), the metric assessed to support Soil PFI, there was considerable disagreement, especially for the higher burn severity classes, with BAER-SBS overestimating the burn severity of ~ 40% of FIA plots in the unburned-low Soil PFI category (> 85% OMC). Approximately 45% of the plots in the low Soil PFI class (< 85% to ≥ 40% OMC) were classified as moderate or high burn severity. In the moderate Soil PFI class (< 40% to ≥ 0% OMC), there was > 40% misclassification representing both overestimates and underestimates of burn severity. Finally, BAER-SBS underestimated the burn severity of ~ 15% of plots that were assessed in the field as having 0% OMC post-fire (Fig. 8).

The distribution of tree biomass mortality proportion to MTBS-assigned burn severity class also indicated some degree of correspondence; however, large

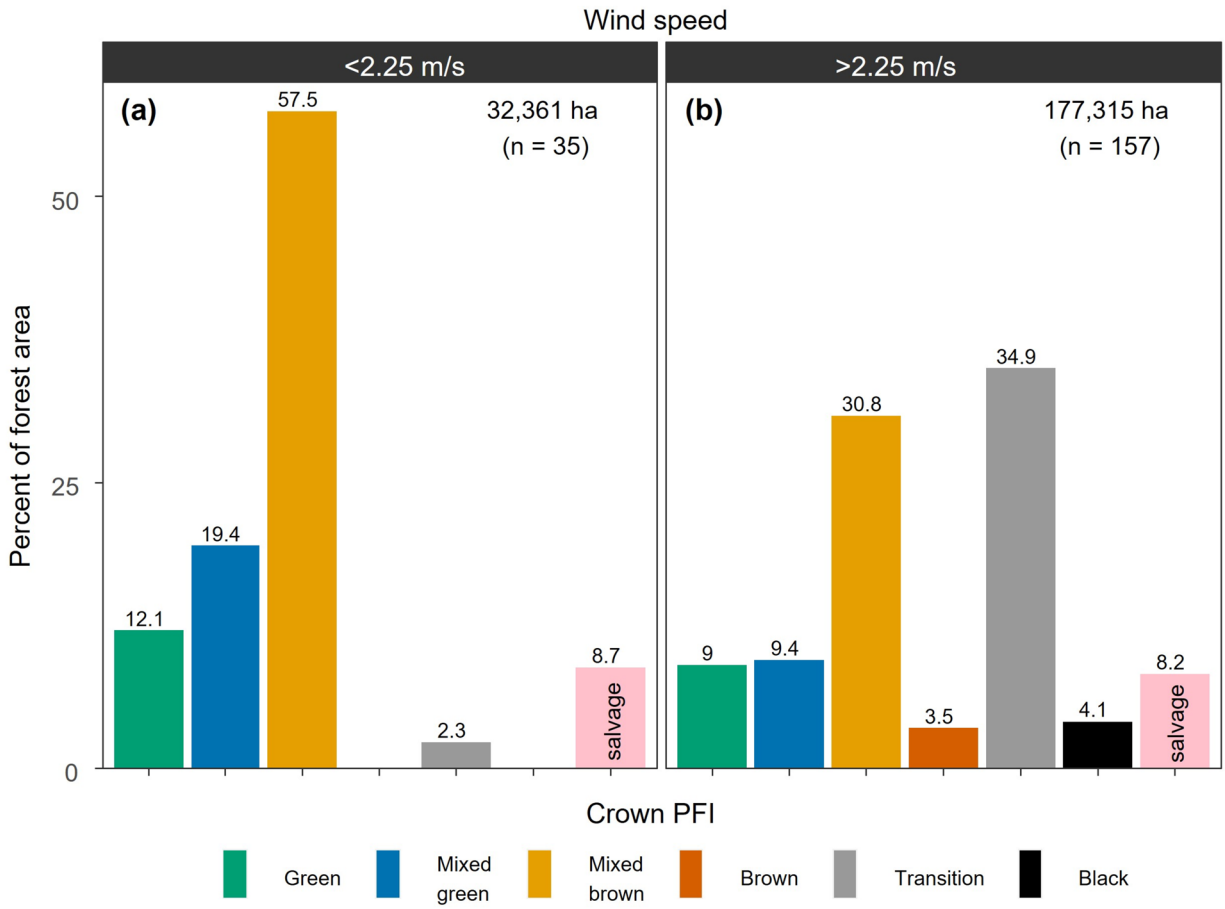

Fig. 6 Distribution of forested area by post-fire crown index (Crown PFI), calculated from crown outcomes for trees > 12.4 cm (> 5 in) diameter for the six 2020 megafires in Oregon and southwest Washington for area represented by Forest Inventory and Analysis (FIA) conditions for which (**a**) wind speed did not exceed 2.25 m/s (5 mph) when fire arrived and (**b**) wind speed was at least 2.25 m/s. The bars labeled salvage represent the forest area that experienced post-fire salvage, such that Crown PFI is indeterminate. Forest area and FIA condition count for each wind speed class and Crown PFI are posted at the top of these charts

discrepancies (> 30%) were observed in the unburned, low, and moderate classes. For plots falling on area classified by MTBS as low burn severity (1–25% expected tree mortality), nearly a third had mortality rates exceeding 25% and 10% experienced tree biomass mortality rates greater than 75%. In forest area classified as moderate burn severity (> 25% to < 75% expected tree mortality), about a quarter of plots were observed to have burned at low burn severity (< 25% mortality) and more than a third at high severity (> 75% mortality). Less than a quarter of plots within area classified as high severity had rates of mortality below 75% (Fig. 9).

Discussion

The FIA pre-fire and FERS post-fire inventory remeasurement data from the 2020 Labor Day Fires, processed and compiled for this study, were exceptionally well-suited to generating statistical estimates of the impact of these fires across a large, forested landscape. They also provide a unique testbed for hypotheses concerning the drivers of fire effects in mesic forests of the western Cascades and serve as a rare basis of empirical, objective, and unbiased "ground truth" against which predictions of modeled fire effects and severity can be evaluated. Given that high winds figured prominently in the spread and behavior of these fires, and that wind speed also varied over these fires' spatial and temporal extents, our characterization of plot-local modeled mean wind speeds circa the arrival of a fire front at each plot provided an opportunity to control for wind speed, revealing empirical evidence of relationships between site factors like age and stand structure and fire effects that were not apparent without such control. As a warming climate elevates fire activity in the western Cascades, we anticipate that this dataset can and will be used to inform a broad range of policy-relevant questions concerning how managers

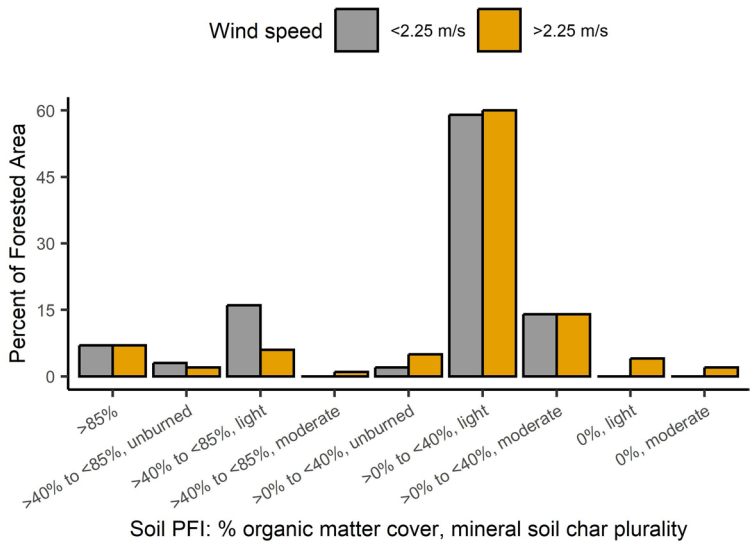

Fig. 7 Post Fire Soil Index (Soil PFI) as percent of forest area that was not subject to salvage and that burned under light winds (< 2.5 m/s; 32,361 ha) and moderate-strong winds (≥ 2.5 m/s; 177,315 ha) at the estimated time of fire arrival, for all six 2020 megafires in Oregon and southwest Washington

might effectively enhance resistance to stand-replacing fire when choosing and implementing silvicultural prescriptions in these forests under moderate (i.e., dry fuels, low winds) to severe (i.e., dry fuels, high winds) fire weather. As these plots continue to be remeasured in the coming decades, the data collected will have much to teach us about how management might promote fire resilience when resistance is futile.

Influence of wind and forest structure on fire effects

At broad scale (both stand- and landscape-level), fire spread, intensity, and severity are commonly understood as outcomes of fuels, topography, and weather (popularly known as the "fire triangle"; Agee 1996). When forest fuels are plentiful, as is typical for productive forests of the western Cascades, weather conditions, specifically a combination of dry fuels and high winds, are widely understood to be a force that dominates and overwhelms the influence of forest structure (Agee 1993; Bessie and Johnson 1995; Agee 1997). In an echo of past high severity megafires in the western Cascades (e.g., the 1902 Yacolt Fire), severe fire weather, in the form of both high fuel aridity and strong, easterly winds, largely accounts for the size and severity of the 2020 Labor Day Fires (Reilly et al. 2022). When modeling drivers of high-severity fire (> 75% overstory tree mortality) via remote sensing across the 2020 Labor Day Fires, Evers et al. (2022) detected that at least one aspect of forest structure (overstory canopy height) was influential in reducing fire severity under periods of high winds. Weather in their analysis was accounted at the daily, not hourly scale, however.

In this study that utilized field-measured data, modeled hourly mean wind speeds > 2.25 m/s (which we reference as moderate to strong) were associated with relatively low tree biomass survival, regardless of tree size (< 25 cm, 25–53 cm, > 53 cm DBH; Fig. 2). One aspect of forest structure appeared to elevate tree survival under moderate to strong winds, however: stand age. Stands for which the predominant tree size class was determined to consist of trees that were 60 to 120 years in age exhibited statistically greater survival compared to those where stand age exceeded 120 years and exhibited median survival rates well above both < 60 and > 120-year-old stands (Fig. 5). In the same vein, under moderate to strong winds, even-aged stands dominated by mid-sized trees (23–51 cm DBH) exhibited greater mean and median tree survival than other structure classes, although high variability prevented detection of statistically significant differences among structure classes (Figure S1).

Under light winds (< 2.25 m/s) but high fuel aridity, forest structure strongly influenced tree survival, where increasing tree size was associated with greater mean and median tree survival; survival was also statistically greater in 60–120-year-old stands than in < 60-year-old stands. These results suggest that management practices that manipulate stand structure in western Cascades forests may have the capacity to enhance stand-level fire resistance under increasingly common moderate (dry fuels but low winds) and to a measurable, but lesser degree under more infrequent, severe fire weather

Table 3 Estimated means and standard errors (SE) of the carbon density (stocks per unit area) in 1) live trees, pre-fire, 2) live trees, post-fire, 3) fire-killed trees, immediately post-fire, and 4) the subset of fire-killed trees that were harvested via salvage logging within 1-year post-fire, by ownership and stand age class

Ownership group	Stand age class (years)							
	1–60		61–120		> 120		All age classes	
	Total	SE	Total	SE	Total	SE	Total	SE
	Megagrams CO_2e per ha from pre-fire tree measurements, post-fire tree status							
National forest								
Pre-fire live	197	31	567	60	574	76	430	38
Post-fire live	102	25	266	59	215	69	188	31
Fire-killed	95	22	299	52	354	61	240	30
Salvaged	0	0	5	5	15	15	6	5
BLM								
Pre-fire live	267	30	739	90	971	88	614	67
Post-fire live	119	34	186	39	435	132	236	54
Fire-killed	148	41	553	95	536	143	378	67
Salvaged	0	0	0	0	35	35	11	11
State								
Pre-fire live	136	22	281	281	687	57	278	56
Post-fire live	99	30	0	0	100	100	70	41
Fire-killed	38	26	281	281	587	587	208	84
Salvaged	0	0	0	0	0	0	0	0
Private								
Pre-fire live	180	19	622	163	–	–	184	20
Post-fire live	50	10	96	80	–	–	49	10
Fire-killed	129	19	526	120	–	–	134	19
Salvaged	72	16	303	303	–	–	75	16
All Owners								
Pre-fire live	191	15	592	49	683	63	344	20
Post-fire live	70	9	222	42	268	61	130	15
Fire-killed	120	14	369	44	412	58	213	17
Salvaged	46	10	23	18	19	13	36	7

conditions (dry fuels and high winds). While an expanding body of literature supports our finding that young forests (e.g., < 60 years old) exhibit minimal fire resistance (e.g., Zald and Dunn 2018), the result that 60–120-year-old stands exhibited greater fire resistance than older (> 120-year-old) stands is surprising, given the conventional wisdom that older forests tend to have the most fire-resistant individuals (e.g., thick barked Douglas-fir trees). Investigation of how key fire-relevant forest structure metrics differed among the three stand age classes revealed that in comparison to > 120 year-old stands, 60–120-year-old stands exhibited (1) a greater canopy base height (i.e., fewer ladder fuels), (2) lower proportion of canopy area in trees with live branches below a critical height above the ground (6.1 m; 20 ft), (3) lower down wood fuel loads, and (4) a similar quadratic mean diameter (i.e., trees [especially Douglas-fir] large enough to exhibit fire resistant characteristics). Further investigation could find other aspects of 60–120-year-old stands that make them more fire resistant under both moderate and severe fire weather conditions to address the policy relevant question of whether and how silvicultural treatments can initiate, accelerate, and/or maintain the resistant structural elements of such stands over time.

Starkly different structures, and potentially, the fire effects they imply, can be seen among ownerships, owing primarily to differences in objectives (e.g., to generate timber revenue vs. ecosystem services, like habitat and recreation, that may sometimes depend on maintaining higher inventories). Tree survival was greater on national forests and BLM forests than on private forests when winds were light (median tree biomass survival rate of 0.85 vs. 0.26; Fig. 4), a finding consistent with Evers et al. (2022) remote sensing-based analysis. Differences in

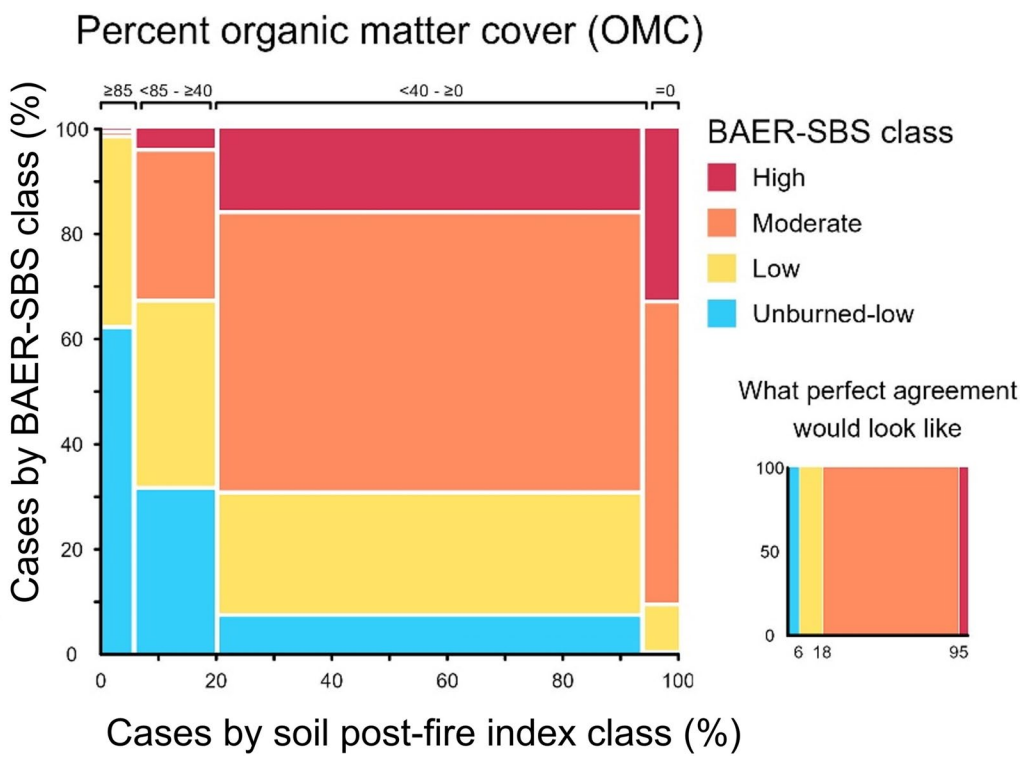

Fig. 8 Comparison of the four classes of percent soil organic matter cover (OMC) observed on the ground to Burned Area Emergency Response Soil Burn Severity (BAER-SBS) classes estimated via remote sensing. The width of each column indicates the proportion of the four soil OMC classes (indicated as brackets at the top), and color represents how burn severity was classified by the BAER-SBS assessment for the same area of the fire. Inset graph indicates how perfect agreement between percent OMC and BAER-SBS classes would present visually. Observations are for plots with a single forested condition where condition proportion exceeds 85% ($n = 130$)

survival among ownerships were not significant where winds were moderate to strong. In the western Cascades, most private forest land is managed to produce timber suitable as feedstock for the manufacture of harvested wood products, with forests typically managed as young (< 60-year-old) even-aged Douglas-fir plantations (Table 1). Under the high fuel aridity and light wind combination increasingly common in late summer, plantations lack the fire resistance found in older, more structurally heterogenous stands common on Federal lands (Zald and Dunn 2018). The positive association of survival with latitude (Fig. 3) may be explained by both differences in ownership and associated forest structure (less private land in the Riverside and Big Hollow fires) and climate (negative association of temperature and aridity with latitude).

Tree survival is often relied on as an integrative proxy for fire effects on forest ecosystems, including impacts on soils and forest cover, despite the sometimes-weak association among those effects. For example, the degree of consumption of organic matter atop and below the soil surface does not necessarily track tree mortality or change in canopy cover. The independently derived crown and soil post-fire indices (PFI) enabled exploration of the crown and soil effects separately in terms of their relationship with wind speed. Under light winds, most of the burned area (89%) retained at least some live trees with green foliage (the green, mixed green, mixed brown classes). Under moderate to strong winds, a sizeable proportion (42.5%) of burned area contained no live trees (brown, transition, black classes). As trees shed fire-killed foliage, loadings of fine and coarse wood may be substantially greater in stands with Crown PFI classified as brown, transition, or black as compared to stands classified as green, mixed green, or mixed brown. Stands in these dead Crown PFI classes are likely at greater risk of moderate to high severity fire effects (due to greater fuel loading) should they reburn in the near future. Unlike Crown PFI, it was less obvious that light vs. moderate to strong winds drove major differences in the distribution of soil organic matter cover (Soil PFI) post-fire. Given a large proportion of burned areas (79%) exhibited minimal organic soil cover (< 40%) post-fire, however, these fires have the potential to produce serious, long-lasting impacts via soil erosion and water quality at watershed- to landscape-scales.

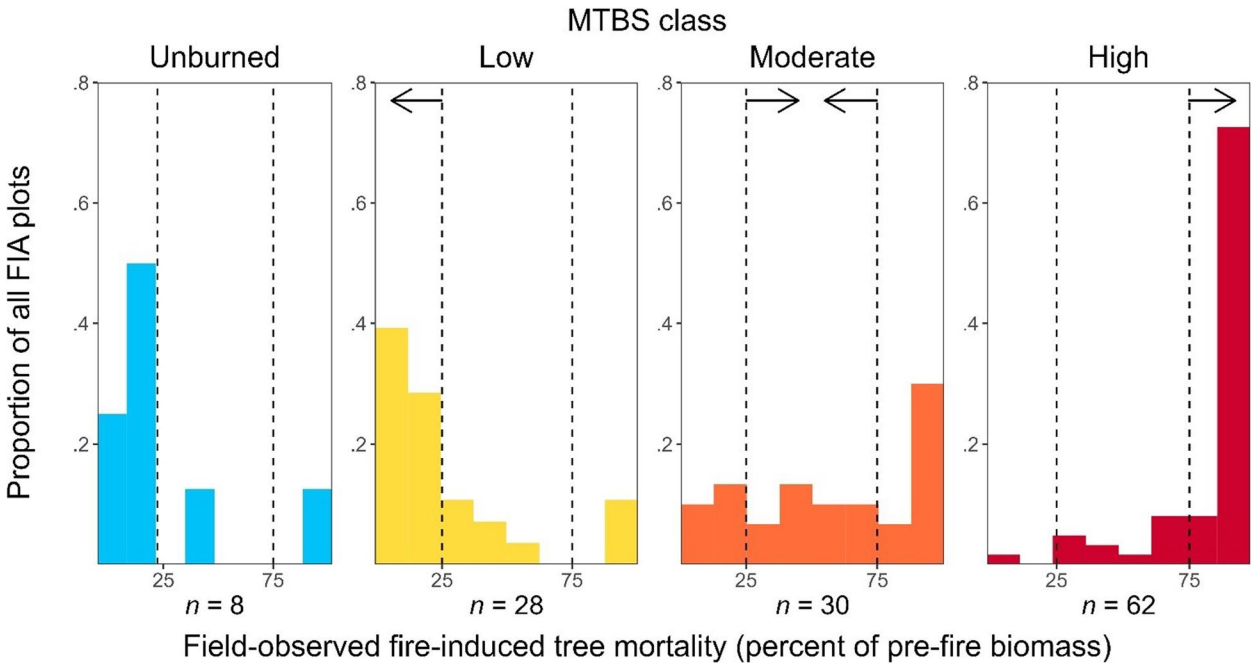

Fig. 9 Distribution of field-observed fire-induced tree mortality, as a percent of pre-fire tree biomass per ha, by Monitoring Trends in Burn Severity (MTBS) assigned burn severity class for 128 Forest Inventory and Analysis (FIA) plots with a single condition greater than 0.85 sampled 1-year post-fire. Dashed lines in each panel denote 25% and 75% observed mortality and the arrows indicate the range in which observed mortality is consistent with the severity class assignments

We expect these results to promote understanding of broad-scale drivers of fire effects in western Cascades forests under conditions like those that prevailed in these east-wind driven fires; however, interpretations might require adjustment when considering drivers of fire effects under the west-winds that are more typical of fire events in this region. Wildfires burning under west-winds may also experience periods of moderate to strong winds (e.g., mean speed > 2.25 m/s), but the speed fluctuations over the hourly time scale for which wind speeds are computed (that produced strong but brief gusts) are much reduced compared to east-wind events, so the incidence and intensity of wind gusts is also reduced. Moreover, moisture content of air in westerlies that originate over the Pacific Ocean is much greater than in the east winds drawn from the continental interior, with very different results for fuel aridity. This is one reason why the Labor Day 2020 Fires burned at such high severity; west-wind fire events in the western Cascades burn more typically at mixed-severity, given the combination of lower fuel aridity and lighter winds (Reilly et al. 2021).

Impact of fire and salvage on carbon

Given that initial stand structures were very different among ownerships, with federal forests containing much older and larger trees (Table 1), variation in live carbon retention—from 25% in state forests to 44% in national forests (Table S4)—was expected. We were surprised that, considering all ownerships combined, carbon retention was almost the same, 37–39%, across all age classes, owing to very different rates of retention within an age class across ownerships. Although the sample size for state forests is small (note a sampling error for this statistic of 1126 gigagrams CO_2e that is 44% of the estimated 2582 gigagram total fire killed CO_2e in Table S4), the 25% overall retention rate on state forests stands out, as does the 72% retention rate on the same ownership in young stands. The latter is in striking contrast with the 28% retention rate on young, privately owned forests—an age class accounting for virtually all forests in that ownership. One possibility is that a larger share of state forest falls within the younger (stand initiation stage) end of the 0–60-year age range while most private forest is between 20 and 60 years old, firmly planted in the stem exclusion stage characterized by continuous canopy closure (Table 1). It is also possible that these ownerships manage their forests at different stand densities or are more or less likely to engage in precommercial thinning and commercial thinning operations.

Live tree carbon retention on national forests was markedly reduced in stands older than 120 years relative to the other age classes and to BLM forests in the same

age class. Additional analysis of the complete dataset may illuminate the extent to which such patterns were driven by where the fire front happened to be during the most severe weather conditions versus differences in forest structure. However, a greater share of the oldest age class is in very old (> 150 years) stands on national forests as compared to BLM and a greater share of BLM forests are in the largest stand size class (Table 1)—a finding consistent with BLM forests having greater site productivity, on average, in western Oregon.

Pre-fire live tree carbon density is much greater on BLM forests. However, the average density of fire-killed carbon on BLM forests is nearly as great as the average density of pre-fire live tree carbon on national forests. This is apparently due to surprisingly low rates of tree survival in all age classes, though particularly in the age class of 60–120 years where survival was 25%. Pre-fire carbon densities in young stands do vary by owner—they are greatest on BLM and least on state forests, with national forests and private forests not significantly different from one another. However, on private and BLM forests, most of the live tree carbon moves to dead pools in these young stands; on national forests, most remains alive. Further analysis is needed to understand how differences in stand structure may account for the differences in outcomes by ownership, to the extent that such drivers can be isolated when fire weather is so influential on survival outcomes.

Considering all ownerships and age classes, the 2020 Labor Day fires produced an enormous carbon transfer out of the live tree pool (Table S4), one that exceeded all anthropogenic atmospheric emissions (from electricity usage, transportation, residential and commercial, industrial and agriculture, combined) in the State of Oregon in the year they occurred (nearly 70 MMT vs 64 MMT CO_2e). It is likely that immediate transfers from the live tree pool to the atmosphere are small (mainly combustion of foliage and fine branches); however, the enormous 70 MMT addition to the dead wood pool has consequentially initiated decades of greatly elevated atmospheric emissions as agents of decay effect a relentless release of the sequestered carbon. Large pools of carbon were immediately released from dead wood, litter, duff, and soils carbon pools; these will be estimated when the full dataset is in hand (including data from plots that were inaccessible in the first year post-fire), and all data are compiled and reconciled to account for growth, removals, and mortality.

Salvage is an important part of this story on private lands. Most of the fire-killed tree biomass was harvested and some share of that converted into long-lived wood products which will prevent release of the stored carbon for a long time. Other salvage components will have been used to generate bioenergy and some share will likely have been left on site to decay or been disposed of via pile burning. Note that the salvage estimates available in this analysis can only account for stands harvested in the first year post-fire. It is likely that additional salvage has occurred since the data was collected from these plots during the first field season following these fires. We hope to account for that activity as data rolls in from future decadal FIA remeasurement visits.

Burn severity product classifications and observed fire effects

Standardized and corporately produced classified burn severity map products derived from the processing of remotely sensed information are regarded as critical decision support for managing post-fire landscapes, especially by managers lacking analytic support to develop their own custom classifications. While easy to access and use, the accuracy of these standardized maps varies, especially over biophysically heterogeneous landscapes (Kolden et al. 2015). Typically derived as a classification of spectral indices (e.g., differenced normalized burn ratio [dNBR]) using a standardized approach that nevertheless contains subjective elements in the parameterization, these burn severity maps recognize four classes: unburned, low, moderate, and high.

To assess accuracy of the predictions implied by burn severity map products, we compared predictions and observations for the spatially balanced sample comprised of burned plots in our FERS data. We evaluated BAER-soil burn severity (SBS) classifications against field-observed ocular estimates of organic matter cover that were collected to determine the top level of the hierarchical Soil PFI classification. We evaluated MTBS-thematic class (TC) classifications against field-observed percent tree biomass mortality. Documentation for the BAER and MTBS products offers qualitative but not strictly quantitative guidance on interpreting what the mapped severity classes mean (Parson et al. 2010; Eidenshink et al. 2007); however, most researchers and managers have long ago adopted what are regarded as conventionally understood quantitative interpretations of these classes. For example, severity is typically mapped to overstory tree mortality as follows: unburned ➔ little to no mortality, low ➔ more than zero but < 25% tree mortality, moderate ➔ 25–75% mortality, and high ➔ > 75% mortality (Miller et al. 2009).

When comparing BAER-SBS and the top-level Soil PFI classes (that correspond to organic matter cover classes), we found a broad spectrum of BAER-SBS class predictions for each field-observed organic soil cover class, especially for what organic matter cover suggests should be low, moderate, and high burn severity (Fig. 8). Given that BAER-SBS uses the dNBR spectral index, an index

constructed to detect change in vegetation (Miller and Thode 2007), not soils, it is perhaps unsurprising that we observed poor agreement between BAER-SBS and Soil PFI's organic matter cover classes. In a comparison of the performance between Landsat-derived spectral burn severity indices and field observations across a broad biophysical gradient, Harvey et al. (2019) found that indices (including dNBR) were better at classifying change to forest canopies than forest floor attributes, such as soils. Furthermore, a field validation study conducted in western Montana and southern California (Hudak et al. 2004) found the BAER-BARC product to be a better predictor of change in vegetation than of soil impacts. While the BAER-SBS product is refined from the raw BARC product with the help of field observations that are essentially used to adjust dNBR thresholds (Parson et al. 2010), dNBR remains the underlying spectral index and key driver of the classification. Given that the BAER-SBS product is commonly used in a wide variety of post-fire landscape risk-assessments (e.g., for transportation, human health and safety, property damage, water quality, invasive species, habitat, soil erosion and landslide potential), the considerable disconnect between SBS classifications and field observations of soil impact observed in this study should throw a cautionary flag for managers concerning whether BAER-SBS is capable of providing credible answers, which will depend very much on their questions. In the western Cascades, at least, the imprecision implied by Fig. 8 may produce disappointing outcomes for decisions reliant on severity characteristics to represent soil vulnerability outcomes post-fire.

The MTBS-TC product is a go-to resource for managers planning post-fire responses (e.g., salvage logging, roadside hazard reduction, replanting, and ecosystem rehabilitation) and by researchers to understand patterns of vegetation and tree mortality due to fire effects at broad scale. However, many researchers choose not to rely on the TC product, implementing, instead, their own analysis and field validation to classify MTBS continuous dNBR values into burn severity classes, onto which they map quantitative interpretations (e.g., Miller and Thode 2007; Miller et al. 2009; Cansler & McKenzie 2012). Referencing the conventionally understood percent tree mortality thresholds quoted earlier, we found that while MTBS-TC classifications across burned FIA plots somewhat tracked these field-observed tree mortality thresholds, observed tree mortality fell outside those thresholds across 25–60% of plots, depending on burn severity class (Fig. 9). Burn severity classifications were most accurate in the high, followed by the low class and worst in the moderate class, where observed tree mortality ranged from 5 to 100% and more than half of plots had observed mortality outside the range associated with moderate severity. Other studies report low accuracy for tree mortality classification under moderate burn severity; classification uncertainty and error tend to be greatest in the intermediate range of spectral index values (Furniss et al. 2020). A large proportion of plots classified as unburned exhibited percent tree mortality far above 0%, raising considerable doubt about the accuracy of fire effects detection by remotely sensed burn severity products, especially when fire induces minimal mortality in overstory trees. This result has important implications for the mapping of fire refugia via remote sensing, given the popular description of fire refugia as unburned islands (e.g., Martinez et al. 2019). Fire refugia with closed canopies may experience significant fire-induced mortality of trees in the mid- and under-story tree canopy layers, not to mention consumption of down wood and understory vegetation—effects that are not detected by remote sensing, particularly when the temporal period of analysis is short (i.e., delayed tree mortality within fire refugia from understory fire effects may eventually emerge > 1-year post-fire; Busby and Holz 2022). As with the BAER-SBS product, it is important that managers (and researchers) be aware that MTBS-TC burn severity classes may poorly represent tree mortality responses to fire in the western Cascades (Whittier and Gray 2016) and that they not uncritically accept its predictions in situations where it is important to have accurate mortality information.

Future work and opportunities

This paper reported a timely and compelling, statistically based summary of short-term outcomes of the 2020 Labor Day Fires and selected examples of the kinds of questions to which data from fire effects enhanced FIA remeasurement protocols data can be applied. This dataset will be augmented with immediate post-fire remeasurement data from ten more plots, whose visitation was deferred a year by post-fire closures, and with formal remeasurement compilation and reconciliation of pre- and post-fire data to provide a basis for precise accounting of growth, mortality, and removals between visits, enhancing its analytical power. As remeasurement data is collected from these FIA plots over the next decade and beyond, post-fire ecosystem trajectories can be tracked with respect to dead wood dynamics (that influence both reburn potential and habitat quality), reestablishment and growth of trees and understory vegetation, carbon fluxes among pools, and effects of post-fire management (e.g., salvage logging and rehabilitation efforts). In the short-term, key opportunities that could be explored, even before post-post-fire remeasurement data become available include (1) modeling the relationship between pre-fire forest structure and observed fire effects to support the development of silvicultural treatments

that enhance fire resistance, (2) validation and refinement of models that predict fire effects and remotely sensed burn severity classifications, and (3) utilization of crown and soil post-fire indices to describe or test fire impacts on phenomena not analyzed here (e.g., riparian or avian habitat quality and their relationships to species abundance).

Even before the 2020 Labor Day Fires, FERS 1- or 2-year post-fire measurements have been collected across a large network of 998 burned (including a subset of reburned) FIA and National Forest System Regional Intensification plots, across California, Washington, and Oregon since 2002. These data have been used, for example, to evaluate modeled, fire induced tree mortality (Barker et al. 2019) and post-fire surface fuel dynamics (Eskelson and Monleon 2018). All these plots have had a post-fire FERS visit, and most have also had at least one post-post-fire standard FIA remeasurement visit, making them a great resource for exploring the post-fire ecosystem trajectory topics described above. This larger FERS dataset represents a significant and forward-looking investment in data collection that, with additional investment in data compilation, reconciliation, quality assurance, and analysis, should be well-positioned to address a great many questions about fire in west coast US forests and the interactions between fire and pre- and post-fire management.

Supplementary Information

The online version contains supplementary material available at https://doi.org/10.1186/s42408-023-00219-x.

Additional file 1: Figure S1. Distribution of the proportion of surviving tree biomass (post-fire live biomass/pre-fire live biomass) by stand structure class and modeled plot-local wind speed class at fire arrival. Metrics represented are means (black circles), medians (black horizonal bars), 95% confidence intervals (black vertical line), and "n" which references the number of forested conditions on which trees were present in the associated fire event and tree diameter class. Statistical differences are indicated by letter assignments among groups in each tree diameter class (Wilcoxon rank sum test; $\alpha = 0.05$). To control for the structural variability different forest types can exhibit, only Douglas-fir dominated stands are presented here (164 out of 215 total conditions). **Figure S2.** Distributions of five forest structure metrics that relate to fire effects and behavior, by stand age class, within the 2020 Labor Day fires. Means are represented by black circles, medians by black bars, and 95% confidence intervals by a black vertical line. Statistical differences for a structure metric are indicated by different tree diameter class letter assignments (Wilcoxon rank sum test; $\alpha = 0.05$). **Table S1.** Pre-fire tree species composition (volume m^3 and proportion of total volume) by fire and all fires combined. **Table S2.** Key for assigning stand-level soil post-fire index (PFI) based on ocular estimates of organic matter cover and mineral soil char class plurality.**Table S3.** Summary statistics (mean and standard deviation [SD]) of important weather variables at time when fire hit the plot. **Table S4.** Estimated totals and standard errors (SE) of carbon stocks in live trees, pre- and post-fire, and in fire-killed trees, immediately post-fire, and in trees harvested via salvage logging within 1-year post-fire by ownership and stand age class. Proportion entries (Prop) on post-fire live lines are survival proportions relative to pre-fire live tree carbon. Proportion entries on salvaged lines are the proportion of carbon in fire-killed trees that were removed from the forest via salvage with 1-year post-fire. **Table S5.** Comparison of areal proportions in hectares and percent between the post fire soil index, classified by field observations of organic matter cover and bare soil char characteristics for each fire and two remotely sensed burn severity metrics: Monitoring Trends in Burn Severity Thematic Class (MTBS-TC) and Burned Area Emergency Response Soil Burn Severity (BAER-SBS). Spatial extents were calculated in a GIS using remotely sensed raster data within the finalized fire perimeters.

Acknowledgements
We are immensely grateful for the invaluable assistance of B. Morefield, M. Palmer, and H. Hayden of the Region 6 Inventory Program and the inventory data collection contractors they worked with—without their tireless efforts in the face of exceptional logistical challenges posed by a pandemic and a massively disrupted post-fire environment, this data would not exist. The USDA Forest Service is a member of the Northwest Regional Modeling Consortium, under the management of C. Mass at University of Washington, which provided the Weather Research Forecasting Model data, with assistance from B. Potter, that allowed us to link weather to the plot locations at the time fire arrived. Additionally, we thank O. Kuegler for his assistance developing a custom stratification of FIA plots for this analysis and the PNW FIA Data Collection and Information Management teams that supported this data collection effort and database development.

Authors' contributions
AK and JF compiled the raw pre- and post-fire FIA data and calculated the fire effect indices. The fire weather analysis that derived estimated wind speed at each FIA plot during fire arrival was led by AK with assistance from SB and JF. SB compiled the analysis database. AK and SB analyzed the fire effect index responses and remotely sensed burn severity product evaluations with assistance from JF. JF analyzed the carbon data. SB drafted the manuscript with assistance and editing from JF and AK. JF supervised the study plan and scope. All authors read and approved the final manuscript.

Funding
Funding to support data collection was received from an Oregon Dept. of Forestry Partnership in Planning Program, USDA Forest Service Region 6, arranged by M. Palmer, the Bureau of Land Management, arranged by K. Ford, and the USDA Forest Service PNW Research Station's Westside Fire Research Initiative, arranged by M. Rollins. This research was supported in part by appointments to the United States Forest Service (USFS) Research Participation Program administered by the Oak Ridge Institute for Science and Education (ORISE) through an interagency agreement between the U.S. Department of Energy (DOE) and the U.S. Department of Agriculture (USDA). ORISE is managed by ORAU under DOE contract number DE-SC0014664. The findings and conclusions in this paper are the responsibility of the authors and should not be construed to represent any official view, determination or policy of the USDA, DOE, ORAU/ORISE or any other U.S. Government entity.

Availability of data and materials
The data that support the findings of this study are available from the USDA Forest Service Forest Inventory and Analysis (FIA) program, but restrictions apply to the availability of these data and so not all data are publicly available. All but exact plot location data for visits to these plots conducted pre-fire are downloadable, as are post-fire visit data collected on scheduled FIA panels (https://apps.fs.usda.gov/fia/datamart/datamart.html). Exact plot locations are not publicly available owing to confidentiality requirements under the Food Security Act, and 1-year post-fire data are not yet available, but eventually will be, because they were collected for and are being analyzed under special studies conducted by the USDA Forest Service PNW Research Station's Westside Fire Research Initiative and its partners.

Declarations

Ethics approval and consent to participate
Not applicable.

Consent for publication
Not applicable.

Competing interests
The authors declare that they have no competing interests.

Author details
[1]Pacific Northwest Research Station, United States Department of Agriculture Forest Service, Portland, OR 97204, USA.

Received: 17 April 2023 Accepted: 12 September 2023
Published online: 10 October 2023

References

Abatzoglou, J. T., D. E. Rupp, L. W. O'Neill, and M. Sadegh. 2021. Compound Extremes Drive the Western Oregon Wildfires of September 2020. *Geophysical Research Letters* 48(e2021GL092520):1–9.

Agee, J.K. 1993. *Fire Ecology of Pacific Northwest Forests*. Washington D.C: Island Press.

Agee, J. K. 1996. The Influence of Forest Structure on Fire Behavior. In Proceedings of the 17th Forest Vegetation Management Conference, 52–68. Redding, CA https://www.fs.usda.gov/rm/pubs/rmrs_gtr292/1996_agee.pdf.

Agee, J.. K.. 1997. The severe weather wildfire-Too hot to handle? *Northwest Science* 71 (1): 5.

Barker, J.S., J.S. Fried, and A.N. Gray. 2019. Evaluating model predictions of fire induced tree mortality using wildfire-affected forest inventory measurements. *Forests* 10 (11): 958.

Bechtold, W. A., and P. L. Patterson. 2005. The Enhanced Forest Inventory and Analysis Program National Sampling Design and Estimation Procedures. Asheville: U.S. Department of Agriculture, Forest Service, Southern Research Station. 85p. https://www.fs.usda.gov/treesearch/pubs/20371.

Bessie, W.C., and E.A. Johnson. 1995. The relative importance of fuels and weather on fire behavior in subalpine forests. *Ecology* 76 (3): 747–762.

Bland, J.M., and D.G. Altman. 1995. Multiple significance tests: The Bonferroni method. *BMJ* 310: 170. https://doi.org/10.1136/bmj.310.6973.170.

Burrill, Elizabeth A.; DiTommaso, Andrea M.; Turner, Jeffery A.; Pugh, Scott A.; Menlove, James; Christiansen, Glenn; Perry, Carol J.; Conkling, Barbara L. 2021. The Forest Inventory and Analysis Database: database description and user guide version 9.0.1 for Phase 2. U.S. Department of Agriculture, Forest Service. 1026 p. [Online]. Available at web address: https://www.fia.fs.usda.gov/library/database-documentation/.

Busby, S. U., and A. Holz. 2022. Interactions between fire refugia and climate-environment conditions determine mesic subalpine forest recovery after large and severe wildfires. *Frontiers in Forests and Global Change* 5 (890893): 1–18.

Cansler, C.A., and D. McKenzie. 2012. How robust are burn severity indices when applied in a new region? Evaluation of alternate field-based and remote-sensing methods. *Remote Sensing* 4 (2): 456–483.

Eidenshink, J., B. Schwind, K. Brewer, Z.-L. Zhu, B. Quayle, and S. Howard. 2007. A project for monitoring trends in burn severity. *Fire Ecology* 3 (1): 3–21.

Eskelson, B.N.I., and V.J. Monleon. 2018. Post-fire surface fuel dynamics in California forests across three burn severity classes. *International Journal of Wildland Fire* 27 (2): 114.

Evers, C., A. Holz, S. Busby, and M. Nielsen-Pincus. 2022. Extreme winds alter influence of fuels and topography on megafire burn severity in seasonal temperate rainforests under record fuel aridity. *Fire* 5 (41): 16.

Franklin, J. F., and C. T. Dyrness. 1973. *Natural Vegetation of Oregon and Washington*. PNW-8: U.S. Dept. of Agriculture, Forest Service, Pacific Northwest Research Station.

Furniss, T.J., V.R. Kane, A.J. Larson, and J.A. Lutz. 2020. Detecting tree mortality with Landsat-derived spectral indices: Improving ecological accuracy by examining uncertainty. *Remote Sensing of Environment* 237: 111497.

Halofsky, J.E., D.L. Peterson, and B.J. Harvey. 2020. Changing wildfire, changing forests: The effects of climate change on fire regimes and vegetation in the Pacific Northwest, USA. *Fire Ecology* 16 (1): 4.

Halofsky, J.. S., D.. R.. Conklin, D.. C.. Donato, J.. E. Halofsky, and J.. B. Kim. 2018a. Climate change, wildfire, and vegetation shifts in a high-inertia forest landscape: Western Washington, U.S.A. ed. C. Carcaillet. *PLOS ONE* 13 (12): e0209490.

Halofsky, J.S., D.C. Donato, J.F. Franklin, J.E. Halofsky, D.L. Peterson, and B.J. Harvey. 2018b. The nature of the beast: Examining climate adaptation options in forests with stand-replacing fire regimes. *Ecosphere* 9 (3): e02140.

Harvey, B.J., R.A. Andrus, and S.C. Anderson. 2019. Incorporating biophysical gradients and uncertainty into burn severity maps in a temperate fire-prone forested region. *Ecosphere* 10 (2): e02600.

Hudak, A. T., R. Forester, P. R. Robichaud, J. S. Evans, J. Clark, K. Lannom, P. Morgan, and C. Stone. 2004. Field validation of Burned Area Reflectance Classification (BARC) products for post-fire assessment. In *Proceedings of the tenth Forest Service remote sensing applications conference*. Salt Lake City, UT: American Society of Photogrammetry and Remote Sensing.

Jain, T.B., D.S. Pilliod, R.T. Graham, L.B. Lentile, and J.E. Sandquist. 2012. Index for characterizing post-fire soil environments in temperate coniferous forests. *Forests* 3 (3): 445–466.

Jain, Theresa B.; Graham, Russell T. 2007. The relation between tree burn severity and forest structure in the Rocky Mountains. In: Powers, Robert F., tech. editor. Restoring fire-adapted ecosystems: proceedings of the 2005 national silviculture workshop. Gen. Tech. Rep. PSW-GTR-203, Albany, CA: Pacific Southwest Research Station, Forest Service, U.S. Department of Agriculture: 213–250

Klock, A. M., S. Busby, and J. S. Fried. 2023. It's about Time: A Method for Estimating Wildfire Arrival and Weather Conditions at Field-Sampled Locations. *Fire* 6 (360):18.

Kolden, C. A., A. M. S. Smith, and J. T. Abatzoglou. 2015. Limitations and utilisation of Monitoring Trends in Burn Severity products for assessing wildfire severity in the USA. *International Journal of Wildland Fire* 24 (7):1023–1028.

Linley, G. D., C. J. Jolly, T. S. Doherty, W. L. Geary, D. Armenteras, C. M. Belcher, R. Bliege Bird, A. Duane, M. Fletcher, M. A. Giorgis, A. Haslem, G. M. Jones, L. T. Kelly, C. K. F. Lee, R. H. Nolan, C. L. Parr, J. G. Pausas, J. N. Price, A. Regos, E. G. Ritchie, J. Ruffault, G. J. Williamson, Q. Wu, D. G. Nimmo, and B. Poulter. 2022. What do you mean, 'megafire'? *Global Ecology and Biogeography* 00 (geb.13499):1–17.

Maechler, M.P., R.A. Struyf, M. Hubert, and K. Hornik. 2021. cluster: Cluster analysis basics and extensions. *R Package Version* 2 (1): 2.

Martinez, A.J., A.J.H. Meddens, C.A. Kolden, E.K. Strand, and A.T. Hudak. 2019. Characterizing persistent unburned islands within the Inland Northwest USA. *Fire Ecology* 15 (1): 20.

Mass, C.F., D. Ovens, R. Conrick, and J. Saltenberger. 2021. The September 2020 Wildfires over the Pacific Northwest. *Weather and Forecasting* 36 (5): 1843–1865.

Miller, J.D., and A.E. Thode. 2007. Quantifying burn severity in a heterogeneous landscape with a relative version of the delta Normalized Burn Ratio (dNBR). *Remote Sensing of Environment* 109 (1): 66–80.

Miller, J.D., E.E. Knapp, C.H. Key, C.N. Skinner, C.J. Isbell, R.M. Creasy, and J.W. Sherlock. 2009. Calibration and validation of the relative differenced Normalized Burn Ratio (RdNBR) to three measures of fire severity in the Sierra Nevada and Klamath Mountains, California, USA. *Remote Sensing of Environment* 113 (3): 645–656.

Parson, A., P. R. Robichaud, S. A. Lewis, C. Napper, and J. T. Clark. 2010. *Field guide for mapping post-fire soil burn severity*. Ft. Collins, CO: U.S. Department of Agriculture, Forest Service, Rocky Mountain Research Station. https://www.fs.usda.gov/treesearch/pubs/36236.

R Core Team. 2022 R: A language and environment for statistical computing. R Foundation for Statistical Computing, Vienna, Austria. URL https://www.R-project.org/).

Reilly, M. J., J. E. Halofsky, M. A. Krawchuk, D. C. Donato, P. F. Hessburg, J. D. Johnston, A. G. Merschel, M. E. Swanson, J. S. Halofsky, and T. A. Spies. 2021. Fire Ecology and Management in Pacific Northwest Forests. In Fire Ecology and Management: Past, Present, and Future of US Forested Ecosystems, Managing Forest Ecosystems., eds. C. H. Greenberg and B. Collins, 393–435. Cham: Springer International Publishing https://www.fs.usda.gov/research/treesearch/63690.

Reilly, M. J., A. Zuspan, J. S. Halofsky, C. Raymond, A. McEvoy, A. W. Dye, D. C. Donato, J. B. Kim, B. E. Potter, N. Walker, R. J. Davis, C. J. Dunn, D. M. Bell, M. J. Gregory, J. D. Johnston, B. J. Harvey, J. E. Halofsky, and B. K. Kerns. 2022. Cascadia Burning: The historic, but not historically unprecedented, 2020 wildfires in the Pacific Northwest. *Ecosphere* 13 (6). https://onlinelibrary.wiley.com/doi/10.1002/ecs2.4070.

USDA Forest Service PNW Research Station FIA, 2021. FIRE EFFECTS AND RECOVERY STUDY- Supplement to Field Instructions for the Annual Inventory of California, Oregon, and Washington 2021. On file at PNW-FIA and at https://www.fs.usda.gov/pnw/documents-and-media/2021-pnw-fia-ca-or-wa-fire-effects-and-recovery-field-manual.

USDA Forest Service PNW Research Station FIA. 2022. Field Instructions for the Annual Inventory of California, Oregon, and Washington 2022. On file at PNW-FIA and at https://www.fs.usda.gov/pnw/documents-and-media/2022-pnw-fia-caorwa-field-manual.

USDA. 2022. Web Soil Survey. Atlanta, GA: US Department of Agriculture. https://websoilsurvey.nrcs.usda.gov/app/.

USGS. 2022. Post-Fire Mapping Glossary. US Geological Survey. https://burnseverity.cr.usgs.gov/glossary.

Whittier, T.R., and A.N. Gray. 2016. Tree mortality based fire severity classification for forest inventories: A Pacific Northwest national forests example. *Forest Ecology and Management* 359: 199–209.

Woodall, C.W.; Heath, L.S.; Domke, G.M.; Nichols, M.C. 2011. Methods and equations for estimating aboveground volume, biomass, and carbon for trees in the U.S. forest inventory, 2010. General Technical Report NRS-88. Newtown Square, PA: U.S. Department of Agriculture, Forest Service, Northern Research Station. 30 p. http://www.treesearch.fs.fed.us/pubs/39555.

Zald, H.S.J., and C.J. Dunn. 2018. Severe fire weather and intensive forest management increase fire severity in a multi-ownership landscape. *Ecological Applications* 28 (4): 1068–1080.

Publisher's Note